HHS Public Access

Author manuscript

Cell Stem Cell. Author manuscript; available in PMC 2019 August 02.

Published in final edited form as:

Cell Stem Cell. 2018 August 02; 23(2): 252–265.e8. doi:10.1016/j.stem.2018.06.001.

Id1 Ablation Protects Hematopoietic Stem Cells from Stress-Induced Exhaustion and Aging

Satyendra K. Singh[1,6,7], **Shweta Singh**[1,7], **Stephen Gadomski**[1], **Lei Sun**[1], **Alexander Pfannenstein**[1], **Magidson Valentin**[2], **Xiongfong Chen**[3], **Serguei Kozlov**[4], **Lino Tessarollo**[1], **Kimberly D. Klarmann**[1,5], and **Jonathan R. Keller**[1,5,8,*]

[1]Mouse Cancer Genetics Program, Center for Cancer Research, NCI. Frederick, MD 21702, USA. [2]Optical Microscopy and Analysis Lab, and [3]Advanced Biomedical and Computation Sciences, and [4]Center for Advanced Preclinical Research, and [5]Basic Science Program, and Leidos Biomedical Research Inc. Frederick National Laboratory for Cancer Research, Frederick, MD 21702, USA. [6]Department of Stem Cell and Cell Culture, Center for Advanced Research, King George's Medical University, Lucknow, India, 226003 [7]These authors contributed equally [8]Lead Contact

SUMMARY

Defining mechanisms that maintain tissue stem cells during homeostasis, stress and aging, is important for improving tissue regeneration and repair, and enhancing cancer therapies. Here we show Id1 is induced in hematopoietic stem cells (HSCs) by cytokines that promote HSC proliferation and differentiation, suggesting that it functions in stress hematopoiesis. Genetic ablation of Id1 increases HSC self-renewal in serial bone marrow transplantation (BMT) assays, correlating with decreases in HSC proliferation, mitochondrial biogenesis, and ROS production. $Id1^{-/-}$ HSCs have a quiescent molecular signature and harbor less DNA damage than control HSCs. Cytokines produced in the hematopoietic microenvironment after γ-irradiation induce Id1 expression. $Id1^{-/-}$ HSCs display a blunted proliferative response to such cytokines and other inducers of chronic proliferation including genotoxic and inflammatory stress, and aging, protecting them from chronic stress and exhaustion. Thus, targeting Id1 may be therapeutically useful for improving HSC survival and function during BMT, chronic stress, and aging.

eTOC:

*Correspondence: kellerjo@mail.nih.gov).

DECLARATION OF INTERESTS

The authors declare no competing interests.

DATA AND SOFTWARE AVAILABILITY

The accession number for the RNA-seq data in this paper is GEO: GSE114533.

SUPPLEMENTAL INFORMATION

Supplemental information includes seven figures and three tables.

Singh et al. show that Id1 is an important mediator of stress hematopoiesis. They found that Id1 deletion protects HSCs from exhaustion in multiple paradigms of chronic and physiologicallyrelevant stress and promotes their quiescence, suggesting that targeting Id1 may improve HSC survival and function during chronic stress and aging.

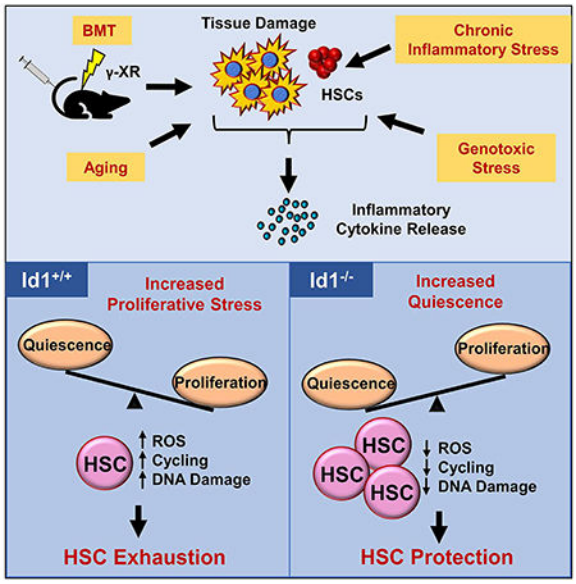

Keywords

Stem cells; hematopoiesis; self-renewal; quiescence; Id proteins; proliferative stress; bone marrow transplantation; aging

INTRODUCTION

Hematopoiesis is an excellent vertebrate developmental system to study adult stem cell biology, and to uncover mechanism(s) that regulate tissue stem cell quiescence, proliferation, self-renewal, cell fate and differentiation (Orkin and Zon, 2008; Seita and Weissman, 2010). Most hematopoietic stem cells (HSCs) are quiescent under homeostasis, and cycle rarely to selfrenew or differentiate into multipotent progenitors (MPPs), and more committed progenitors, with limited self-renewal potential (Nakamura-Ishizu et al., 2014). Hematopoiesis is tightly regulated by both intrinsic and extrinsic mechanism(s), which balance quiescence, self-renewal and differentiation to maintain normal multi-lineage reconstitution (Mendelson and Frenette, 2014; Morrison and Scadden, 2014). While our knowledge of gene function and their mechanism(s) of action has greatly expanded, the precise pathways that maintain HSC quiescence, and prevent HSC exhaustion and subsequent bone marrow failure, remain to be fully elucidated.

Inhibitor of DNA binding (*Id1*-4) proteins are helix-loop-helix (HLH) transcription factors that lack a basic region found in other family members, which is required for DNA binding (Ling et al., 2014; Perk et al., 2005). Id proteins bind to ubiquitously expressed basic(b)HLH E proteins and disrupt their ability to bind DNA, thus inhibiting their transcriptional activity.

E proteins are required for proper differentiation and cell cycle arrest of adult muscle, neural, endothelial, and hematopoietic lineage cells (Kee, 2009; Wang and Baker, 2015). As key regulators of E proteins, Id proteins have been implicated in neural, epithelial, and hematopoietic stem and progenitor cell proliferation and self-renewal (Lasorella et al., 2014). Id proteins are often deregulated in human cancers, where they contribute to tumor growth, invasiveness, metastasis, and self-renewal of cancer stem cells (CSCs) (Lasorella et al., 2014; Perk et al., 2005). Thus, a complete understanding of the function of Id genes in normal adult stem cells and CSCs could lead to the development of novel therapies.

Mice that lack *Id1* (*Id1*$^{-/-}$) develop normally and show no overt phenotypes; however, these mice have dysregulated hematopoiesis which includes decreased bone marrow cellularity, increased hematopoietic progenitor cycling, decreased B cell numbers, and increased myeloid cell output in the bone marrow (Jankovic et al., 2007; Perry et al., 2007; Suh et al., 2009). These phenotypes are due, in part, to cell non-autonomous effects of *Id1* in the hematopoietic microenvironment (HME), since *Id1*$^{-/-}$ bone marrow cells (BMCs) show normal development when transplanted into γ-irradiated (γIR) *Id1*$^{+/+}$ recipient mice (Suh et al., 2009). The number of HSCs are roughly the same in *Id1*$^{-/-}$ and *Id1*$^{+/+}$ under homeostasis and *Id1* is expressed at low levels in HSCs, suggesing that *Id1* may not be required to maintain HSCs during steady-state hematopoiesis. However, *Id1* is induced in HSPCs by growth factors that promote myeloid proliferation and differentiation including IL-3, and enforced expression of *Id1* in HSPCs promotes myeloid proliferation, implicating *Id1* as a potential modulator of HSC function, including proliferation, self-renewal and differentiation under conditions of hematopoietic stress (Cochrane et al., 2009; Leeanansaksiri et al., 2005; Suh et al., 2008). Therefore, we examined the intrinsic role of *Id1* in HSC stress using serial bone marrow transplantation (BMT) assays.

We found that *Id1*$^{-/-}$ HSCs show enhanced self-renewal potential, and are maintained during serial BMT. *Id1*$^{-/-}$ HSCs show reduced cycling and proliferation and increased quiescence after BMT. *Id1*$^{-/-}$ HSC quiescence is associated with reduced levels of γH2AX phosphorylation, reduced mitochondrial biogenesis and stress, and lower ROS levels. *Id1*$^{-/-}$ HSCs are protected from cytokine-induced proliferative stress *in vitro*. HSCs express low levels of *Id1* under homeostasis; however, *Id1* is induced in HSCs after BMT, in part, by proinflammatory cytokines present in the HME after γIR. *Id1*$^{-/-}$ HSCs are protected from exhaustion by other conditions that model chronic physiological stress including toll-like receptor (TLR) signaling and aging.

RESULTS

Hematopoietic stem cells that lack *Id1* have enhanced self-renewal potential.

Since *Id1* is induced in HSPCs by cytokines *in vitro,* and overexpression of *Id1* promotes HSPC proliferation (Cochrane et al., 2009; Suh et al., 2008), we hypothesized that *Id1* may have an important function in stress hematopoiesis. First, we backcrossed conventional Id1 knockout mice (*Id1*$^{-/-}$) maintained on a mixed B6;129 background with C57BL/6 mice for ten generations, to study mice on a pure genetic background. We found that the cell-non autonomous hematopoietic phenotype previously reported for *Id1*$^{-/-}$ mice on the mixed background to be less severe on the pure C57BL/6 background (Suh et al., 2009).

Specifically, loss of *Id1* in the C57BL/6 background did not result in differences in myeloid and lymphoid cell development in peripheral blood cells (PBCs) or BMCs (Figures S1A-B). In addition, the previously observed reduction in BM cellularity was not as pronounced (Figure S1C), the increase in lineage-negative Sca-1^{+}c-Kit^{+}(LSK) and HSPC populations was less severe (Figure S1D-E), and no effect on HSC numbers was observed (Figure S1E, and summarized Figure1F). We performed competitive serial repopulation assays to evaluate the function of *Id1*$^{-/-}$ BMCs, and found that mice transplanted with *Id1*$^{+/+}$ BMCs did not survive beyond the fourth serial BMT due to HSC exhaustion, while donor *Id1*$^{-/-}$ BMCs survived a fourth, fifth and sixth BMT, and succumbed to exhaustion after the seventh BMT (Figure 1A). This observation was confirmed using noncompetitive serial BMTs, in which *Id1*$^{+/+}$ BMCs failed to support hematopoiesis after the third BMT, while *Id1*$^{-/-}$ donor derived BMCs survived through tertiary transplantation. The *Id1*$^{-/-}$ BMCs failed to promote the survival of quaternary BMT recipient mice (Figure S2A). Collectively, these data suggest that *Id1*$^{-/-}$ HSCs have enhanced self-renewal potential.

To understand how *Id1*$^{-/-}$ HSCs are maintained during serial BMT, we examined donor cell engraftment by flow cytometry. No statistically significant differences in the percentage of donor reconstitution in primary recipients transplanted with *Id1*$^{+/+}$ or *Id1*$^{-/-}$ BMCs was observed, suggesting that *Id1*$^{-/-}$ and *Id1*$^{+/+}$ BMCs contain roughly equivalent numbers of HSCs (Figure 1B). No differences in lineage development were found, other than the expected decreased percentage of mature B cells, previously reported for *Id1*$^{-/-}$ mice (Figure 1C) (Cochrane et al., 2011). However, donor reconstitution was significantly decreased in second and third serial recipients that received *Id1*$^{+/+}$ BMCs, and the fourth serial transplant recipients did not survive. Strikingly, *Id1*$^{-/-}$ donor BMC engraftment was sustained through 7 serial transplants, suggesting that *Id1*$^{-/-}$ HSCs have enhanced self-renewal potential (Figure 1B). As predicted, the total number of donor-derived HSCs was roughly equivalent in primary *Id1*$^{+/+}$ and *Id1*$^{-/-}$ BMT recipients 14 weeks after BMT (Figure 1D-E and Figure S2B). However, donor *Id1*$^{-/-}$ HSCs were significantly increased in the 2nd and 3rd BMT recipient mice compared to *Id1*$^{+/+}$ HSCs, and gradually declined in serially transplanted mice, but were sustained through six serial BMTs. Recipients of the fourth *Id1*$^{+/+}$ BMT failed to reconstitute due to exhaustion of donor HSCs. Additional immunophenotypic analysis using antibodies that recognize CD34, confirmed that *Id1*$^{+/+}$ HSCs were significantly decreased in the 2nd and 3rd serial BMT recipients, while *Id1*$^{-/-}$ HSCs were maintained through six serial BMTs (Figure 1E). No difference in the homing of *Id1*$^{-/-}$ and *Id1*$^{+/+}$ Lin^{-}, LSK, or HSCs was observed, suggesting alternative mechanism(s) for the increased self-renewal of *Id1*$^{-/-}$ HSCs (Figure S2C). Thus, *Id1*$^{-/-}$ HSCs have enhanced self-renewal potential and are maintained during serial BMT with normal lineage developmental potential and homing function.

Loss of *Id1* in HSCs could affect the development of progenitors downstream of HSCs; therefore, we analyzed HSPC populations in secondary BMT recipients. As expected, we observed an increase in the number of donor HSCs and ST-HSCs in mice transplanted with *Id1*$^{-/-}$ BMC; however, there were no detectable differences in MPPs (Figure S2D). Thus, while the total number of *Id1*$^{-/-}$ HSCs were higher in secondary BMT recipient mice compared to *Id1*$^{+/+}$ recipients, the number of committed MPPs was the same, suggesting a critical function for *Id1* in HSCs under conditions of BMT related stress.

Hematopoietic stem cells that lack *Id1* show increased quiescence after bone marrow transplantation

Ionizing radiation (γ-IR) is used to condition patients that receive BMT; however, γ-IR induces a proinflammatory cytokine storm and increases the production of reactive oxygen species (ROS), promoting DNA damage in hematopoietic and HME cells (Kim et al., 2014). Quiescent donor HSCs are induced to proliferate and differentiate in primary γ-IR recipients, and serial BMT eventually leads to bone marrow failure and aplasia due to HSC exhaustion. Since *Id1* promotes HSPC proliferation (Leeanansaksiri et al., 2005), and replication stress can drive the functional decline of HSCs (Beerman et al., 2013; Flach et al., 2014; Walter et al., 2015), we examined the proliferative status of $Id1^{-/-}$ HSCs in primary BMT recipient mice. $Id1^{-/-}$ HSCs, but not $Id1^{-/-}$ STHSCs and $Id1^{-/-}$ MPPs, showed a significant increase in G0, and a reduction in G1 and S/G2/M, compared to $Id1^{+/+}$ HSCs 12–14 weeks after BMT, indicating that fewer $Id1^{-/-}$ HSCs are in cycle compared to $Id1^{+/+}$ HSCs (Figure 2A and Figure S3A). We compared HSC cycling 4 and 8 weeks after BMT, and found that few donor $Id1^{+/+}$ and $Id1^{-/-}$ HSCs were in G0 4 weeks after BMT, and most (>90%) were in G1 and S/G2/M (Figure S3B). There was a decrease in the number of $Id1^{-/-}$ HSCs in G1 compared to $Id1^{+/+}$ BMCs, and a trend toward an increase in the number of $Id1^{-/-}$ HSCs in G0. In comparison, 8 weeks after BMT, there are increased numbers of $Id1^{-/-}$ and $Id1^{+/+}$ HSCs in G0; however, there is a significant decrease in the number of $Id1^{-/-}$ HSCs in S/G2/M and an increase in G1 compared to $Id1^{+/+}$ HSCs (Figure S3B). Taken together, $Id1^{-/-}$ HSCs show decreased cycling that begins 4–8 weeks after BMT, and is maintained for 3–4 months after BMT, suggesting that $Id1^{-/-}$ HSCs show prolonged resistance to proliferative stress after BMT.

Since DNA replicative stress is accompanied with γH2AX phosphorylation at stalled replication forks (Branzei and Foiani, 2010; Flach et al., 2014; Walter et al., 2015), we measured the phosphorylation of histone H2AX S139 phosphoyrlation (γH2AX) in $Id1^{-/-}$ HSCs 12–14 wks after BMT. Flow cytometry analysis of $Id1^{-/-}$ HSCs showed a significant reduction in γH2AX levels compared with $Id1^{+/+}$ HSCs, suggesting that $Id1^{-/-}$ HSCs accumulated less DNA damage after BMT in primary recipient mice (Figure 2C). $Id1^{-/-}$ HSCs showed reduction in γH2AX 4 weeks after BMT, indicating that this occurs relatively early after BMT (Figure S3C). Photomicrographs of γH2AX stained HSCs show reduced γH2AX phosphorylation in $Id1^{-/-}$ HSCs compared to $Id1^{+/+}$ HSCs (Figure 2D). To validate the specificity of γH2AX staining, we analyzed levels of γH2AX phosphorylation in host versus donor Lin^- cells in primary recipient mice. As expected, the level of γH2AX staining was higher in host cells, which received a lethal dose of γIR compared to the non irradiated donor cells (Figure S4A). Examination of another marker of DNA damge, 53BP1, showed increased 53BP1 flourescence in $Id1^{-/-}$ HSCs compared to $Id1^{+/+}$ in HSCs 12 weeks after BMT (Figure S4B). Recent evidence suggests that 53BP1 binding is increased on unreplicated DNA, while newly replicated DNA shows reduced 53BP1 binding (Pellegrino et al., 2017). Thus, the increased 53BP1 floursecence that we observe in $Id1^{-/-}$ HSC directly correlates with reduced replicative stress and increased quiescence.

Furthermore, we provide evidence that the reduced cell cycling and DNA damage in *Id1*$^{-/-}$ HSCs does not lead to increased cell death, as no difference in the number of apoptotic and dead cells was observed in *Id1*$^{-/-}$ and *Id1*$^{+/+}$ transplanted HSPCs (Figure S4C).

To rule out that *Id1* has direct role in DNA damage repair, *Id1*$^{+/+}$ and *Id1*$^{-/-}$ purified BMCs (Lin^{-} or LSK) were cultured for 16 hours in serum free media with mSCF and hTPO, exposed to 6 Gy γ-IR, then analyzed for γH2AX staining after 1, 4.5 and 24 hours (Figure S4D). No differences in the percentages of γH2AX^{+} cells were detected during the 24-hour period, indicating that *Id1*$^{+/+}$ and *Id1*$^{-/-}$ Lin^{-} and LSK cells have similar repair kinetics after γ-IR, and suggest no direct role for *Id1* in DNA damage repair. Thus, the reduced levels of γH2AX phosphorylation in *Id1*$^{-/-}$ HSCs compared to *Id1*$^{+/+}$ after serial BMT is not a direct effect of *Id1* in the DNA damage response. Rather, the data suggest that the levels of γH2AX phosphorylation reflect reduced replication stress and increased quiescence of *Id1*$^{-/-}$ HSC during serial BMT. Thus, loss of *Id1* reduces replicative stress, thereby helping to preserve the number and function of *Id1*$^{-/-}$ HSCs during serial BMT.

Since *Id1*$^{-/-}$ HSCs show reduced cycling after BMT, we asked if *Id1*$^{-/-}$ HSCs might proliferate less in other *in vivo* models of chronic proliferative stress. Therefore, we examined serial administration of a sublethal dose of 5-fluorouracil (5-FU) to chimeric *Id1*$^{-/-}$ and *Id1*$^{+/+}$ mice, which induces chronic proliferative stress, stem cell exhaustion and bone marrow failure (Harrison and Lerner, 1991). We observed a significant delay in 5-FU induced hematopoietic failure in *Id1*$^{-/-}$ recipients, where 50% of the *Id1*$^{-/-}$ mice survived a third administration of 5-FU, while most *Id1*$^{+/+}$ recipient mice did not survive beyond the second 5-FU treatment (Figure 2E). HSPC analysis of BMCs from chimeric mice treated with 5-FU (2x) confirm that BMCs from mice transplanted with *Id1*$^{-/-}$ BMCs contain roughly twice as many donor HSCs as mice transplanted with *Id1*$^{+/+}$ BMCs (Figure 2F). In addition, the *Id1*$^{-/-}$ HSCs show a significant reduction in proliferation compared to *Id1*$^{+/+}$ cells, as measured by BrdU incorporation assays (Figure 2G). Finally, BMCs from 5-FU-treated *Id1*$^{-/-}$ mice show increased donor repopulation in competitively transplanted mice 12 weeks after BMT (Figure S4E), and give rise to increased numbers of immunophenotypic HSCs compared to *Id1*$^{+/+}$(Figure S4F). This suggests that there are increased numbers of of functional HSCs after 5-FU treatment in chimeric *Id1*$^{-/-}$ mice. These results are consistent with the interpretation that *Id1*$^{-/-}$ HSCs remain quiescent after 5-FU induced proliferative stress compared to *Id1*$^{+/+}$ HSCs, and thus, are able to provide hematopoietic protection from serial 5-FU-induced proliferative stress.

Id1$^{-/-}$ HSCs show reduced mitochondrial and cellular stress after bone marrow transplantation

HSCs induced to proliferate *in vitro* and *in vivo* show increased mitochondrial biogenesis, increased mitochondrial stress, and increased reactive oxygen species (ROS) generation, which damage DNA and can lead to functional exhaustion of HSCs (Flach et al., 2014; Walter et al., 2015). Therefore, we examined the metabolic activity of *Id1*$^{-/-}$ and *Id1*$^{+/+}$ HSCs in secondary BMT recipient mice, since these mice show a significant difference in the number of HSCs. *Id1*$^{-/-}$ HSCs, but not ST-HSCs or MPPs, showed reduce mitochondrial biogenesis compared to *Id1*$^{+/+}$ HSCs after BMT (Figure 3A). Furthermore, *Id1*$^{-/-}$ HSCs

showed reduced mitochondrial stress compared to *Id1*$^{+/+}$ HSCs by JC-1 fluorescent staining, which measures mitochondrial membrane depolarization (Figure 3B). Recent studies indicate that HSCs with low mitochondrial membrane potential are enriched for HSCs with increased competitive repopulation ability (Sukumar et al., 2016; Vannini et al., 2016). We observed a significant decrease in ROS production in *Id1*$^{-/-}$ HSCs compared to *Id1*$^{+/+}$ HSCs (Figure 3C), which agrees with reduced mitochondrial metabolic activity of *Id1*$^{-/-}$ HSCs (Figure 3B). Finally, *Id1*$^{-/-}$ HSCs show significantly higher levels of reduced thiols, known to correlate with reduced glutathione levels, as indicated by ThiolTracker Violet staining (Figure 3D). Collectively, these data show that *Id1*$^{-/-}$ HSCs have reduced mitochondrial biogenesis and metabolic activity, less ROS production, and reduced signs of oxidative stress. Together, these results are consistent with the proposed model that *Id1*$^{-/-}$ HSCs are more quiescent and resistant to BMT-induced hematopoietic stress.

Since *Id1* is expressed at low levels in HSCs, and is induced under conditions of replicative stress, we hypothesized that absence of *Id1* would show little effect on HSCs during steady-state hematopoiesis. Therefore, we examined mitochondrial biogenesis/stress and ROS production in *Id1*$^{+/+}$ and *Id1*$^{-/-}$ HSCs under homeostasis. No difference in mitochondrial biogenesis, and mitochondrial stress, as measured by Tetramethyrhodamine methyl ester (TMRM) staining was observed in *Id1*$^{-/-}$ and *Id1*$^{+/+}$ HSCs in young (2 month) and middle aged (1 year) mice (Figure S5B-C). In addition, no difference in ROS production was observed in *Id1*$^{-/-}$ and *Id1*$^{+/+}$ HSCs in young mice; however, we observed reduced levels of ROS in middle aged *Id1*$^{-/-}$ HSCs compared to *Id1*$^{+/+}$ HSCs (Figure S5A). Thus, no differences in mitochondrial biogenesis/stress or production of ROS is observed in young and middle aged *Id1*$^{-/-}$ and *Id1*$^{+/+}$ HSCs under homeostasis, except that *Id1*$^{-/-}$ HSCs from middle aged mice show reduced ROS production compared to *Id1*$^{+/+}$ HSCs.

Id1 is induced in HSCs after bone marrow transplantation and by proinflammatory cytokines

Id1 mRNA is expressed at low levels in LSK cells, with elevated levels observed in committed myeloid progenitors (CMPs, GMPs, and neutrophils) (Leeanansaksiri et al., 2005; Perry et al., 2007), suggesting that steady-state levels of *Id1* are low in HSPCs, and increase during normal myeloid differentiation. Myeloid growth factors, including interleukin-3 (IL-3), have been shown to induce expression of *Id1* mRNA in LSK, and overexpression of *Id1* in normal HSPCs promotes proliferation (Cochrane et al., 2009; Suh et al., 2008). Thus, we reasoned that *Id1* may be induced in HSCs by the cytokine storm produced in the HME after γIR, which promotes HSC proliferation and hematopoietic reconstitution (Kim et al., 2014; Schaue et al., 2012). To measure induction of *Id1* expression in HSCs, we used *Id1*-GFP reporter knock-in mice (*Id1*$^{GFP/+}$), which accurately reports *Id1* expression in normal BMCs (Perry et al., 2007). We confirmed that HSCs, ST-HSCs, and MPPs expressed low levels of *Id1*(GFP), and that *Id1*(GFP) expression increases in GMPs, MEPs and neutrophils (Figure 4A). BMCs from *Id1*$^{GFP/+}$ mice were cultured in serum free medium containing cytokines or known proinflammatory agents for 36 hours, and then examined for *Id1*(GFP) expression in HSCs by flow cytometry. SCF did not induce *Id1*(GFP) expression in HSCs, while SCF with IFNγ, TPO, IL-6, or LPS induced high levels of *Id1*(GFP) expression. SCF plus IL-3, GM-CSF, FLT3L, pI:pC, IL-1β, IFNα, or

TNFα induced comparatively lower levels of GFP expression in HSCs (Figure 4B). To confirm that GFP expression accurately reflects Id1 protein levels, we purified GFP^{Hi} and $GFP^{Lo/Med}$ cells cultured in SCF/TPO/IFNγ for 36 hours by FACS, and show that Id1 protein levels directly correlate with the level of GFP expression in these cells (Figure S6A). Taken together, HSCs express low levels of *Id1* under steady-state conditions, and *Id1* expression can be increased in these cells by cytokines and inflammatory agents *in vitro*.

We have shown that overexpression of *Id1* transgene in HSPCs promotes progenitor cell proliferation *in vitro* and *in vivo* (Suh et al., 2008). To determine if growth-factor-induced *Id1* expression correlates with increased proliferation, we measured BrdU incorporation in *Id1*(GFP^+) HSCs compared to *Id1*(GFP^-) HSCs. Lin- BMCs from $Id1^{GFP/+}$ reporter mice were cultured in SCF, SCF/TPO or SCF/IFNγ for 48 hours, and then BrdU was added for the last 3 hours of incubation. GFP^+ HSCs show increased BrdU incorporation in cultures containing SCF/TPO and SCF/IFNγ compared to cultures containing SCF alone. In comparison, GFP^- showed significantly less BrdU incorporation (Figure 4C), indicating that cytokine induced *Id1*(GFP) expression correlates with increased proliferation of HSCs.

We hypothesize that radiation-induced damage to the HME can increase *Id1* expression in HSCs; therefore, we treated $Id1^{GFP/+}$ reporter mice with increasing doses of γ-IR and examined GFP expression in HSCs after 48 and 72 hrs. The expression of *Id1*(GFP) in HSCs was upregulated with increasing doses of γIR (4, 6, or 8 Gy) from an average of 7% to 25% 48 hours post γ-IR, and up to 45% 72 hours after treatment (Figure S6B). Further, we examined if the administration of individual cytokines could increase the expression of *Id1*(GFP) in HSCs *in vivo*. To rule out any effect of the $Id1^{-/-}$ HME, we generated chimeric mice by transplanting BMCs from $Id1^{GFP/+}$ reporter mice ($CD45.2^+$) into $Id1^{+/+}$ recipient mice ($CD45.1^+$). Six Gy γIR induced high levels of *Id1*(GFP) in donor HSCs. Administration of IFNγ, pI:pC and, to a lesser extent, IL-6 also induced *Id1*(GFP) expression in HSCs compared to control mice (Figure 4D). Thus, *Id1* expression is induced in HSCs after γIR, and by cytokines produced in the HME after γIR.

Cytokines produced as part of the cytokine storm in the HME after γIR may function alone, or in combination, to induce *Id1* expression in HSCs. Because of the complexity of this milieu, it would be difficult to predict which individual cytokines to knock down to reduce *Id1* induction in HSCs *in vivo*. We previously found that JAK2 inhibitors block IL-3-induced *Id1* expression in the MPP cell line, EML, suggesting that *Id1* is downstream of JAK-2 activation (data not shown). Furthermore, we show here that IFNγ, IL-6, TPO, GM-CSF and other cytokines, which signal through the JAK/STAT pathway also induce GFP (*Id1*). Therefore, we reasoned that treating mice with pan-JAK (momelotinib) or pan-STAT (SH-4–54) inhibitors would inhibit the signaling of multiple cytokines, and would thus inhibit induction of *Id1* expression in HSCs *in vivo*. To test this, mice were pretreated with momelotinib and SH-4–54, exposed γIR, and transplanted with Lin^- $Id1^{GFP/+}$ BMCs, whereby a subsequent analysis of GFP (*Id1*) expression in HSCs was performed (Figure 4E). Momelotinib and SH-4–54 significantly inhibited the induction of GFP (*Id1*) expression in donor LSK and HSCs 48 hours after BMT. This demonstrates that *Id1* is induced in HSCs after BMT in γIR recipient mice, in part, via cytokines that signal through the JAK/STAT pathway.

Id1$^{-/-}$ HSCs are resistant to cytokine-induced proliferative stress *in vitro*

Since *Id1* drives HSPC cycling, and *Id1* induction is downstream of cytokines and inflammatory signals, we speculated that *Id1*$^{-/-}$ HSCs may be protected from cytokine induced proliferation *in vitro*. To test this, we cultured *Id1*$^{-/-}$ and *Id1*$^{+/+}$ LSK cells in cytokine conditions known to promote HSC expansion/proliferation *in vitro*, and determined how many HSCs persist in culture over time (Dahlberg et al., 2011; Walasek et al., 2012). While the total number of HSCs declined in all cultures after 6 days as expected, there were significantly more *Id1*$^{-/-}$ HSCs surviving in culture compared to *Id1*$^{+/+}$ HSCs (Figure 5A and Figure S6C). To determine how *Id1*$^{-/-}$ HSCs are maintained in these cultures, we examined the cycling status of HSCs, and found that half as many *Id1*$^{-/-}$ HSCs were in cycle (6%) compared to *Id1*$^{+/+}$ HSCs (12%) (Figure 5B). Furthermore, we found that *Id1*$^{-/-}$ HSCs are proliferating less after 6 days in culture compared to *Id1*$^{+/+}$ HSCs in BrdU-incorporation assays (Figure 5C). Finally, *Id1*$^{-/-}$ LSK cells cultured for 6 days *in vitro* showed increased donor repopulation in competitive repopulation assays compared to Id1$^{+/+}$ LSK cultured cells, indicating that increased numbers of *Id1*$^{-/-}$ HSCs are maintained in LSK cultures after 6 days (Figure S6D). These results are consistent with the interpretation that *Id1*$^{-/-}$ HSCs proliferate and differentiate less in response to cytokines *in vitro*, which may be a part of the mechanism by which the *Id1*$^{-/-}$ HSCs maintain their presence and function during serial BMT.

To confirm that *Id1*$^{-/-}$ HSCs remain quiescent in these cultures, we measured the proliferation of single *Id1*$^{-/-}$ and *Id1*$^{+/+}$ HSCs sorted into Terasaki plates. Greater than 80% of single *Id1*$^{-/-}$ and *Id1*$^{+/+}$ HSCs did not divide after 24 hours in the two different cytokine conditions tested (Figure 5D). After 48 hours in culture, an average of 50% of the HSCs remained undivided in cultures containing SCF/TPO, and fewer than 30% remained undivided in SCF/TPO/IL-3 cultures (data not shown), since addition of IL-3 is a stronger proliferative signal, with no observed difference between *Id1*$^{+/+}$ and *Id1*$^{-/-}$ HSCs. However, 60 hours after the initiation of culture, significantly more *Id1*$^{-/-}$ HSCs remained undivided in cultures containing SCF/TPO (Figure 5D) and SCF/TPO/IL-3 (data not shown) compared to *Id1*$^{+/+}$ HSCs, suggesting that *Id1*$^{-/-}$ HSCs proliferate less in response to cytokines *in vitro.* These data suggest that *Id1*$^{-/-}$ HSCs show increased quiescence and are less responsive to proliferative stimuli, which results in increased surivival *in vitro*.

Id1$^{-/-}$ HSCs are resistant to exhaustion caused by chronic toll-like receptor signaling

Since *Id1*$^{-/-}$ HSCs were protected from the chronic proliferative stress of serial BMT and 5-FU treatment, we asked if *Id1*$^{-/-}$ HSCs might be protected from chronic inflammatory proliferative stress *in vivo*, including prolonged exposure to toll-like receptor (TLR) ligands, lipopolysaccharides (LPS). Repeated exposure to LPS mimics chronic inflammation and results in increased HSC cycling, increased myeloid bias of HSCs, and ultimately, HSC exhaustion, resembling an aging phenotype in mice (Esplin et al., 2011). We treated *Id1*$^{-/-}$ or *Id1*$^{+/+}$ chimeric mice with low dose LPS every other day for 30 days, and found that the absolute number of *Id1*$^{+/+}$ HSCs in LPS-treated mice was significantly reduced compared to untreated mice, confirming that chronic LPS treatment leads to HSC exhaustion. In comparison, the number of *Id1*$^{-/-}$ HSCs in LPS-treated mice was significantly increased

compared to *Id1*$^{+/+}$ HSCs in LPStreated mice (Figure 5E). Thus, *Id1*$^{-/-}$ HSCs are resistant to chronic LPS-induced HSC exhaustion.

Reduced aging of *Id1*$^{-/-}$ HSCs

Aging of the hematopoietic system is associated with increased numbers of myeloid biased CD150-high HSC (CD150^{Hi} HSC) and decreased numbers of lymphoid biased HSCs, CD150low (CD150^{Lo} HSC), decreased repopulation ability of HSCs, and increased DNA damage in HSCs (Beerman et al., 2010a; Beerman et al., 2010b; Geiger et al., 2013; Wahlestedt et al., 2015). Serial BMT, chronic genotoxic (5-FU), and inflammatory stress (LPS) resemble premature aging of the hematopoietic system; therefore, we speculated that HSCs in *Id1*$^{-/-}$ mice might show reduced signs of aging (Beerman et al., 2013; Dykstra et al., 2011). To measure this, we bred *Id1*$^{fl/fl}$ mice (Figure S7A) to male *Tie2-Cre* transgenic mice, which intrinsically deletes *Id1* in HSCs and endothelial cells, but not other cells in the HME, and then compared HSCs in aged (24 month) and young (2 month) *Tie2-Cre*$^{+}$*;Id1*$^{fl/fl}$ (*Tie-2;Id1*$^{-/-}$) and *Tie2-Cre*$^{+}$*;Id1*$^{+/+}$ (*Tie2;Id1*$^{+/+}$) mice. Aged *Tie2;Id1*$^{-/-}$ BMCs show a significant decrease in CD150^{Hi} HSCs (myeloid biased), and an increase in the percentage of CD150^{Lo} HSCs (lymphoid biased) compared to aged *Tie2;Id1*$^{+/+}$ BMCs, which is consistent with an immunophenotype young HSCs (Figure 6A). Total numbers of CD150^{Hi} HSCs were also decreased in aged *Tie2;Id1*$^{-/-}$ mice compared to *Tie2;Id1*$^{+/+}$ mice (Figure S7B). The expression of CD41 (increased on aging HSCs) was decreased on aged CD150^{Hi} and CD150^{Lo} *Tie2;Id1*$^{-/-}$ HSCs compared to aged *Tie2;Id1*$^{+/+}$ HSCs, which is consistent with a youthful immunophenotype of *Tie2;Id1*$^{-/-}$ HSCs (Figure 6B) (Gekas and Graf, 2013). Finally, no difference in myeloid and lymphoid development was observed in PBCs from young *Tie2;Id1*$^{-/-}$ *and Tie2;Id1*$^{+/+}$ mice, while there was an increase in T cells in PBCs from 15 mos *Tie2;Id1*$^{-/-}$ compared to *Tie2;Id1*$^{+/+}$ mice, which is consistent with a youthful phenotype of *Tie2;Id1*$^{-/-}$ HSCs (Figure S7C-D).

To determine if the aged *Id1*$^{-/-}$ HSCs also have improved functional capacity, we transplanted equal numbers of aged *Tie2;Id1*$^{-/-}$ or *Tie2;Id1*$^{+/+}$ HSCs into 10 Gy γIR treated recipient mice, and examined HSC function in serial BMT assays. Although no differences were observed in the survival of primary BMT recipients, aged *Tie2;Id1*$^{-/-}$ HSCs have increased ability to repopulate secondary BMT recipient mice compared to *Tie2;Id1*$^{+/+}$ HSCs, demonstrating that aged *Tie2;Id1*$^{-/-}$ HSCs BMCs have improved HSC function (Figure 6C). We determined the lineage repopulation potential in primary recipient mice, and found that aged *Tie2;Id1*$^{-/-}$ BMCs showed a significant increase in T cell repopulation 4 months after transplantation, but not in B220^{+} B cells (Figure 1B), though *Id1*$^{-/-}$ BMCs have reduced B cell potential in BMT assays (Cochrane et al., 2011). No difference in myeloid repopulation was observed. Thus, aged *Tie2;Id1*$^{-/-}$ HSCs show increased lymphoid-biased HSCs, no myeloid bias, and greatly improved HSC function compared to the aged *Tie2;Id1*$^{+/+}$ BMCs, suggesting that *Id1*$^{-/-}$ HSCs show functional hallmarks of youthful HSCs.

To examine how *Id1*$^{-/-}$ HSCs are protected from functional decline during aging, we compared cell cycling in young and old HSCs by Ki-67 staining. We found no differences in the cycling status of young *Tie2;Id1*$^{-/-}$ and *Tie2;Id1*$^{+/+}$ HSCs, with few HSCs in cell cycle,

as expected (Figure 6D). While the number of HSCs in cycle (S/G2/M) were the same in aged *Tie2;Id1*$^{-/-}$ and *Tie2;Id1*$^{+/+}$ HSCs, we found that the number of aged *Tie2;Id1*$^{-/-}$ HSCs in G0 was increased, while HSCs in G1 were decreased compared to the aged *Tie2;Id1*$^{+/+}$ HSCs (Figure 6D). These data suggest that there are increased numbers of quiescent HSCs in aged *Tie2;Id1*$^{-/-}$ mice.

Since aged *Tie2;Id1*$^{-/-}$ HSCs showed increased quiescence, we asked if these HSCs might also show reduced γH2AX phophorylation. As expected, young *Tie2;Id1*$^{+/+}$ HSCs showed low levels of γH2AX staining, which was not affected by the loss of *Id1* expression; however, the level of γH2AX staining in aged *Id1*$^{-/-}$ CD150^{Hi} and CD150^{Lo} HSCs was significantly lower compared to *Id1*$^{+/+}$ HSCs (Figure 6E). Thus, increased quiescence of aged *Tie2;Id1*$^{-/-}$ HSCs is correlated with reduced phosphorylation of γH2AX. We also evaluated ROS levels in the HSPC of aged *Tie2;Id1*$^{-/-}$ and *Tie2;Id1*$^{+/+}$ since ROS levels increase in aged HSCs, and can affect their function during aging (Ito et al., 2006). We found that ROS levels were significantly lower in aged *Tie2;Id1*$^{-/-}$ HSCs compared with *Tie2;Id1*$^{+/+}$ HSCs (Figure 6F). We showed above that ROS levels are low and similar in young *Id1*$^{+/+}$ and *Id1*$^{-/-}$ HSCs, and are increased in *Id1*$^{+/+}$ HSCs in middle aged (1 year) mice (Figure S5A), and that ROS levels are reduced in middle aged *Id1*$^{-/-}$ HSCs compared to *Id1*$^{+/+}$ HSCs (Figure S5A). Thus, we confirm that ROS levels increase in HSCs as they age, and that *Id1*$^{-/-}$ HSCs are protected from increased ROS levels during aging. Further analysis of conventional mice demonstrate that aged *Id1*$^{-/-}$ HSCs show reduced mitochondrial stress (TMRM^{+}) and mitochondrial biogenesis (Mitotraker green^{+}) compared to *Id1*$^{+/+}$ HSCs, which can account, in part, for the observed decrease in ROS expression in aged mice (Figure S5B-C). Collectively, these data suggest that during aging, loss of *Id1* protects HSCs from increased proliferation, which results in reduced mitochondrial biogenesis/stress and ROS-induced damage, rendering *Id1*$^{-/-}$ HSCs more resistant to functional decline.

Quiescent molecular signature of *Id1*$^{-/-}$ HSC after BMT

To explore the molecular basis by which *Id1* loss promotes HSC quiescence under stress we compared the transcriptome of *Id1*$^{-/-}$ and *Id1*$^{+/+}$ HSCs isolated from primary BMT recipient mice by RNA-seq. We found 179 upregulated and 1476 downregulated genes in *Id1*$^{-/-}$ HSCs compared to *Id1*$^{+/+}$ HSCs using a fold-change cut-off of 2 (Table S1). Ingenuity pathway analysis (IPA) of differentially expressed genes revealed that the Top Biological Functions affected in *Id1*$^{-/-}$ HSCs included, cell stress and injury, protein and gene expression, cell proliferation and growth, and cell signaling, which were all decreased (Figure 7A). The top canonical pathways and networks affected in *Id1*$^{-/-}$ compared to *Id1*$^{+/+}$ HSCs included, Cellular Stress and Injury Pathways (EIF2 Signaling, mTOR signaling, Regulation of eIF4 and p70S6K, AMPK, ATM signaling, NRF2Mediated Oxidative Stress Response), Cell Cycle Pathways, and Cell Signaling Pathways, which were all decreased in *Id1*$^{-/-}$ HSCs (Figure S7E and Table S2 and S3). Collectively, the IPA analysis shows that *Id1*$^{-/-}$ HSCs have gene expression profiles consistent with reduced response to stress, reduced cycling and proliferation, and reduced ribosomal biogenesis and protein synthesis, indicating that *Id1*$^{-/-}$ HSCs have a quiescent molecular signature compared to *Id1*$^{+/+}$ HSCs. GSEA analysis of differentially expressed genes confirmed the IPA analysis, and showed

significantly reduced expression of genes involved in cell cycle and cell division (Cdk2, Cdk6, Wee1, Cyclin D2/D3, PCNA and others) (Figures 7B and S7F), mitochondrial biogenesis and oxidative phosphorylation (Complex IV-cytochrome C oxidase: Cox8A/6A1/6B1, Complex I: NdufA8/V1/V4 and Complex V-ATP Sythase: ATP5F1/ATP5J/ATP5G1) (Figures 7C and S7G), and ribosome biogenesis (Rp12/5/32, Rps6/8/19 and others) (Figures 7D and S7H). Thus, *Id1*$^{-/-}$ HSCs show a quiescent molecular signature including reduced cycling, decreased mitochondrial biogenesis and oxidative phosphorylation, and decreased ribosomal biogenesis which is consistent with the hypothesis that *Id1*$^{-/-}$ HSCs remain quiescent during conditions that promote chronic proliferative stress.

Id1 increases HSC proliferation by antagonizing E protein function.

E-proteins inhibit cellular proliferation by upregulating cyclin dependent kinase inhibitors (CDKI's) (p21, p27, p57, and p16), and Id1 inhibits E-protein function, which results in increased cell proliferation (Lasorella et al., 2014; Roschger and Cabrele, 2017). *E2A*$^{-/-}$ HSCs show decreased expression of *p21* and *p27*, increased HSC cycling, and decreased self-renewal in serial BMT experiments (Semerad et al., 2009; Yang et al., 2011). Furthermore, HSCs that lack *p21* show decreased self-renewal in serial BMT experiments (Cheng et al., 2000). These data suggest that E proteins restrain HSC proliferation, in part, by increasing CDKI gene expression. *Id1*$^{-/-}$ HSCs show decreased proliferation and enhanced self-renewal after BMT; therefore, we speculate that Id1 increases HSC proliferation by antagonizing E protein function (Id1-E2A-CDKI pathway). To test this hypothesis, we evaulated the expression of p21, p27 and p16 in HSCs cultured *in vitro*, and in HSCs after 14 weeks competitive BMT *in vivo*. *Id1*$^{-/-}$ HSCs showed increased expression of p27 and p16 after 6 days in expansion cultures, and increased expression of p21 and p27 after 14 weeks BMT compared to Id1$^{+/+}$ HSCs (Figure 7E-F). Thus, increased CDKI expression in *Id1*$^{-/-}$ HSCs correlates with decreased proliferation of HSCs. Furthermore, knockdown of *E2A* and *p16* using shRNA expressing lentiviral vectors significantly increased the proliferation of *Id1*$^{-/-}$ LSK CD48- HSCs in expansion cultures compared to control shRNA treated cells (Figure 7G). Quantitative RT-PCR confirmed shRNAmediated knockdown of *E2A* and *p16* gene expression in the *Id1*$^{-/-}$ HSC expansion assay *in vitro* (Figure S7I). Taken together, these experiments suggest that Id1 increases HSC proliferation by restraining E protein function, and by reducing p16 expression.

DISCUSSION

Id proteins are expressed at low levels in most tissues and differentiated cell types, but can be induced by a wide array of extracellular signals in response to stress or injury resulting in increased proliferation, growth, tissue repair and regeneration; this suggests that Id genes may be part of the functional response to hematopoietic stress. Since *Id1* expression is induced in HSPC by growth factors that promote proliferation and differentiation, we examined if *Id1* might function in conditions of hematopoietic stress including BMT. We show here that *Id1*$^{-/-}$ HSCs have enhanced self-renewal potential and are protected from exhaustion during serial BMT. Specifically, *Id1*$^{-/-}$ HSCs show reduced cell cycling and proliferation, and reduced DNA damage after BMT. These are indicative of reduced

proliferative stress, and could protect *Id1*$^{-/-}$ HSCs from exhaustion. *Id1*$^{-/-}$ HSCs show a reduction in mitochondrial biogenesis and metabolic activity, reduced intracellular ROS levels, and increased levels of reduced glutathione, which suggests that *Id1*$^{-/-}$ HSCs are more quiescent after BMT *in vivo*. We provide evidence that HSCs express low levels of *Id1* under steady state hematopoiesis. Moreover, cytokines and other proinflammatory stimuli present in the HME after γ-IR can induce *Id1* expression and proliferation in HSCs, suggesting that HSC exhaustion is mediated, in part, by the proinflammatory HME after BMT. Consistent with these observations, we found that administration of pan-JAK and STAT inhibitors, which prevent signaling of many proinflammatory cytokines, partially block *Id1* induction in HSCs after BMT. Furthermore, *Id1*$^{-/-}$ HSCs demonstrate reduced ability to proliferate and differentiate in response to cytokines *in vitro* and after transplantation *in vivo,* while enforced expression of *Id1* promotes HSC proliferation (Suh et al., 2008), suggesting that *Id1* promotes HSC proliferation in response to extracellular signals produced under conditions of hematopoietic stress. BMT stress resembles other chronic stress including chronic exposure of BMCs to IFNs, IL-1, or LPS *in vivo*, which induce stem cell proliferation and exhaustion (Baldridge et al., 2010; Esplin et al., 2011; Pietras et al., 2016; Trumpp et al., 2010). We found that *Id1*$^{-/-}$ HSCs are protected from exhaustion in other models of chronic stress including chronic genotoxic stress (5-FU treatment), chronic inflammatory stress (LPS treatment), and aging, suggesting that reducing *Id1* levels during chronic stress could have therapeutic potential by preserving HSC pools.

Quiescent HSCs with limited divisional history have the greatest repopulating ability, while HSCs that have divided show reduced repopulating ability (Qiu et al., 2014; Sawen et al., 2016). Thus, HSCs that exit dormancy, divide and differentiate, and progressively lose repopulation potential and eventually exhaust. These observations are consistent with the protective function of *Id1* in stress hematopoiesis, whereby *Id1*$^{-/-}$ HSCs show reduced proliferation and increased quiescence *in vitro* and after BMT *in vivo* and, thus, are protected from cell division, differentiation and exhaustion. Under conditions of acute stress, some HSCs are induced to express *Id1*, and are pushed into division to differentiate and enter the active pool of MPPs to provide myeloid cell reconstitution and protection after the stress or injury. After which, hematopoiesis returns to steady-state conditions with minimal loss of HSC function. However, under conditions of chronic stress, *Id1*$^{-/-}$ HSCs have an apparent advantage over *Id1*$^{+/+}$ HSCs and are protected from exhaustion by maintaining quiescence. Interestingly, it has been shown that HSCs maintain a high proliferation rate even 4 months after BMT compared to non-transplanted mice using assays to track the division history of HSCs after BMT, which suggests that the γIR (conditioned) HME may remain damaged long after and BMT resulting in chronic proliferative stress to the transplanted HSCs (Rodrigues-Moreira et al., 2017; Sawen et al., 2016; Schaue et al., 2015). Thus, it would be predicted that inhibiting *Id1* expression in HSCs during BMT, especially in BMTs with poor graft function, or those with concurrent infections, and other situations of chronic stress including aging, might protect the HSC pool from depletion.

Since it is difficult to predict which proinflammatory cytokines produced in the HME after γIR induce *Id1* and promote HSC proliferation; we used small molecule inhibitors of common cytokine signal transduction pathways that target multiple cytokines. We found that inhibitors of the JAK and STAT pathways partially reverse the induction of *Id1* in HSCs

after BMT, confirming that *Id1* is downstream of the JAK/STAT pathway *in vivo*, suggesting that other signal transduction pathways might contribute to the induction of *Id1* to promote HSC proliferation after BMT. For example, we found that LPS induces *Id1* in HSCs, and that $Id1^{-/-}$ HSCs are protected from the chronic inflammatory stress induced by repeated LPS treatment, suggesting a potential role for other TLRs and their ligands in HSC exhaustion during BMT. Thus, we speculate that inhibiting TLRs that recognize pathogen associated molecular patterns (PAMPs) other than LPS, and TLRs that recognize damage-associated molecular patterns (DAMPS), or alarmins, produced after bone marrow conditioning (γIR) and tissue damage might also inhibit *Id1* expression, and protect HSCs from exhaustion during BMT. In support of this hypothesis, BMCs that lack TLR4 or TLR9 show significantly enhanced reconstitution after BMT compared to WT mice (Ichii et al., 2010), suggesting a potential role for these receptors and their downstream signaling pathways in protecting HSCs from chronic stress of BMT. Similarly, since TNF and IL-1 induce *Id1* expression in HSCs, inhibitors of TNFRs, IL-1Rs and possibly IL-8R signaling might also block induction of *Id1* in HSCs. Interestingly, BMCs that lack TNFR-p55 and TNFR-p75 show greatly enhanced competitive serial repopulation ability compared to WT mice during BMT (Markus et al., 2009), suggesting that inhibiting TNFR signaling might protect HSCs during chronic stress. Thus, it will be important in future studies to examine additional small molecule inhibitors of TLRs, TNFRs and other pathways to determine if they prevent *Id1* induction in HSCs, and if they preserve or rescue HSCs from exhaustion during BMT or from other chronic proliferative stress (Matatall et al., 2016; Zhang et al., 2016).

Current methods to expand HSCs *in vitro* for BMT and cell therapy, including gene editing, have been challenging due to the differentiation of the initial stem cell population (Walasek et al., 2012). Recent evidence suggests that HSCs with extensive proliferative history *in vivo* have poor hematopoietic repopulation ability, suggesting that methods to expand HSCs may result in HSC populations with poor function. Therefore, it will be necessary to develop methods that promote HSC survival and expansion without loss of function *in vitro*. Our results show that HSCs that lack *Id1* are preserved in cytokine expansion cultures *in vitro*. Thus, for purposes of gene editing or transgene expression, inhibiting *Id1* function in current expansion media could result in a significant increase in functional HSCs.

In summary, chronic stress from BMT, chronic inflammatory diseases and infections, hematopoietic malignancies, bone marrow failure syndromes, and aging promote HSC exhaustion. The data shown here provide evidence that *Id1* is induced in quiescent HSCs by the proinflammatory HME after BMT, which promotes proliferation, differentiation and hematopoietic reconstitution. However, under conditions of chronic stress, $Id1^{-/-}$ HSCs have an advantage and are protected from proliferative stress by remaining quiescent without losing engraftment and repopulation ability. Thus, moderating levels of *Id1* in HSCs could be therapeutically beneficial under conditions of chronic stress including BMT, bone marrow failure, and chronic inflammatory conditions.

STAR METHODS

KEY RESORUCES TABLE

CONTACT FOR REAGENTS AND SOURCE SHARING

Further information and requests for resources and reagents should be directed to, and will be fulfilled by the Lead Contact, J.R.K. (kellerjo@mail.nih.gov).

EXPERIMENTAL MODEL AND SUBJECT DETAILS

Mice

Id1$^{-/-}$ mice on C57BL/6 background were derived from *Id1*$^{-/-}$ mixed background mice (B6;129 generously provided by Robert Benezra) after 10 (or greater) generations of backcross with C57BL/6 mice (Charles River). *Id1*$^{fl/fl}$ mice were generated by inserting LoxP sequences around exon 2 and 3 by the CCR Gene Targeting Facility, NCI Frederick, MD, USA (summarized in Figure S7A). *Id1*$^{fl/fl}$ mice were bred with male Tie2-Cre^{+} mice (Koni et al., 2001) to generate Tie2-Cre^{+};*Id1*$^{fl/fl}$ (*Tie2;Id1*$^{-/-}$)and Tie2-Cre^{+};*Id1*$^{+/+}$ (*Tie2;Id1*$^{+/+}$) mice. C57BL/6 *Id1*-EGFP knock-in reporter mice (*Id1*$^{GFP/+}$) were generously provided by Xiao-Hong Sun, Oklahoma Medical Research Foundation, Oklahoma, US. C57BL/6 Ly5.2 (CD45.1) mice were obtained from Charles River. All mice were maintained on C57BL/6 genetic background. Recipient mice used in BMT experiments were 8–12 week old females. Experiments involving the use of mice were approved by the NCI at Frederick Animal Care and Use Committee in accordance with the eighth edition “Guide for the Care and Use of Laboratory Animals.”

Chronic LPS treatment

1 × 10^{6} total BMCs from *Id1*$^{+/+}$ and *Id1*$^{-/-}$ mice were transplanted into 10 Gy irradiated CD45.1 recipients. Twenty weeks after BMT, transplanted mice were treated with LPS (Sigma) 0.043 mg/kg every alternate day for 30 days. On the 31st day, mice were euthanized and HSPCs were analyzed as described above.

METHOD DETAILS

Bone marrow transplantation

For competitive serial BM transplantation assays, BMCs (5×10^{5}) from *Id1*$^{+/+}$ and *Id1*$^{-/-}$ mice (CD45.2) were mixed with 5×10^{5} C57BL/6 (CD45.1) BMCs and transplanted into γ-irradiated (10 Gy, ^{137}Cs source) congenic CD45.1 mice by tail vein injection (iv). Recipient mice were pretreated one week before and two weeks after transplantation with antibiotic-containing water (pH 2.5–3.0, 0.5 mg/mL amoxicillin, 0.17 mg/mL enrofloxacin). Donor reconstitution was determined in peripheral blood cells (PBCs) 4 and 8 weeks after BMT, and after 12–14 weeks in PBCs and bone marrow. For serial transplantation experiments, 1 × 10^{6} total BMCs from pooled recipients were transplanted into 10 Gy irradiated secondary recipient, and similarly for the 3rd, 4th, 5th, 6th, and 7th BMT. Donor reconstitution was determined by flow cytometry in PBCs 4 and 8 weeks after BMT, and in the bone marrow and/or peripheral blood after 12 weeks for all BMT recipient mice. HSCs were purified from

aged *Tie2;Id1*$^{-/-}$ or *Tie2;Id1*$^{+/+}$ mice mice by FACS. HSCs (100) CD45.2^{+} were co-transplanted with 1 × 10^{5} CD45.1^{+} radioprotective BMCs into primary γ-IR recipient mice. BMCs from primary recipient mice were pooled, and then transplanted (1 ×10^{6} cells) into secondary recipient mice and mice were monitored for survival (n=5 mice/group). PBCs from primary recipient mice were analyzed for donor lineage reconstitution after 4 months by flow cytometry.

Lineage and hematopoietic stem and progenitor cell analysis

Single-cell suspensions were prepared from *Id1*$^{+/+}$ or *Id1*$^{-/-}$ BMCs or from BMCs and PBCs of animals transplanted with *Id1*$^{+/+}$ or *Id1*$^{-/-}$ bone marrow cells (BMCs). BMCs were harvested from femurs and tibias by flushing with PBS (1% BSA) using 25 gauge needle and syringe. The light density BMC fraction was isolated using lymphocyte separation media (LSM) (MO Biomedicals, LLC., Solon, OH). PBCs collected from mandibular bleed, were incubated with ACK lysis buffer (Lonza) to lyse red cells followed by a wash in staining buffer (1% BSA in PBS). PBCs and BMCs were incubated with the following fluorochrome conjugated monoclonal antibodies for lineage analysis: CD45.2 (104), Mac-1 (M1/70), Gr-1 (RB6–8C5), B220 (RA3–6B2), CD4 (GK1.5), CD8 (53–6.7), CD71 (R17217) and Ter119 (Ter119). For HSPC analysis LSM purified BMCs were treated with Fc receptor blocking antibodies (anti-mouse CD16/32), then incubated with biotinylated lineage markers (Mac-1, Gr-1, B220, TER119, CD4, CD8, and IL-7Rα), and fluorochrome conjugated streptavidin, followed by the addition of directly flourochrome labeled antibodies (as indicated): c-Kit (ACK2), Sca-1(D7), CD150 (mShad150), CD48 (HM48–1), CD34 (RAM34), Flk2 (A2F10), anti-FcγRII/III (FcR) (93). Lin-negative (Lin^{-}) c-Kit^{+} and Sca-1^{+} (LSK) cells were analyzed according to the following marker expression: HSC: LSK Flk2CD150^{+} CD48^{-}, short-term HSC (ST-HSCs): LSK Flk2^{-}CD150^{-}CD48^{-}, and multipotent progenitors (MPP): LSK Flk2^{-}CD150^{-}CD48^{+} and LSK Flk2^{-}CD150^{+}CD48^{+}. All cells were incubated in staining buffer for 45 min on ice with intermittent mixing, and then washed in buffer prior to analysis. All the antibodies used were purchased from BD Biosciences (San Jose, CA) or eBiosciences (San Diego, CA). For annexin V staining, BMCs stained for HSPC analysis were further incubated with annexin V-FITC (BD Biosciences) and analyzed immediately by flow cytometry. For cell cycle/quiescence and DNA damage assays, BMCs stained for HSPC analysis were fixed and permeabilized with Cytofix/Cytoperm buffer (BD Biosciences) followed by intracellular staining overnight with Ki-67-FITC (B56) (BD Biosciences) and γH2AX-PE (20E3) (phosphor Ser139) (Cell Signaling, Danvers, MA) antibody. Cells were incubated with FxCycle Violet dye (ThermoFisher, Waltham, MA) 2–4 hrs before acquisition. BD LSRII SORP and BD Fortessa were used for FACS acquisition and Aria II for cell sorting. Data analysis was done using FlowJo V9 software (Tree Star Inc., Ashland OR). For analysis of cyclin dependent kinase inhibitor expression (CDKI), BMCs stained for HSPC analysis were fixed and permeabilized with BD cytofix/perm buffer, and then blocked with respective purified isotype control antibody for 40 min on ice and then stained with p16 (Santacruz Biotech, sc-166760 PE), p21 (Santacruz Biotech, sc-6246 Alexa fluor 488) and p27 (Santacruz Biotech, sc-1641PE) for 30 min at room temperature and analyzed by flow cytometry.

Immunoflourescence Analysis of HSCs

BMCs were harvested from primary BMT recipient mice 12 weeks after competitive repopulation of *Id1*$^{+/+}$ and *Id1*$^{-/-}$ BMCs. BMCs were further separated using LSM density gradient and stained for HSC cell surface markers. Donor-derived CD45.2^{+} LSK CD150^{+}48- HSCs were isolated from *Id1*$^{+/+}$ and *Id1*$^{-/-}$ transplanted mice by FACS. Approximately 1000 sorted HSCs were incubated for 1 hr. at 37°C in 200ul of Stemspan medium, on retronectin (20ug/ml) coated 8-well chamber slides (Thermo Fischer Scientific). The cells were fixed with 4% paraformaldehyde for 15 min at RT, washed with PBS (3X) and then permeabilized by 0.25% Triton X-100 for 10 min at RT. The cells were then blocked with 10% goat and donkey serum overnight at 4°C. Afterwhich, the cells were incubated with 1:1000 diluted anti-γH2AX (S139) (20E3) (Rabbit, #9718, Cell Signaling Technology), 4°C overnight or anti-53BP1 (Rabbit, Abcam), 4°C overnight. After washing four times with PBST (PBS + 0.1% tween 20) the cells were incubated with 1:2000 diluted Alexa Fluor594 -conjugated goat anti-rabbit IgG(H + L) antibody (Jackson ImmunoResearch laboratories) at RT for 2 hrs. The cells were again washed four times with PBST and counterstained and mounted with Prolong Gold antifade reagent with DAPI (Life Technologies). Cells were imaged on Leica SP8 microscope equipped with Spinning Disk Confocal CSU-W1 (Yokogava) and Zyla4.2 sCMOS camera (Andor), using x63 oil immersion lens. Z-stacks with 0.3um step was acquired over the 12 μm range, so that full Z range was scanned for all cells. Images were processed and analyzed in ImageJ. The antibody signal was normalized to DAPI signal to account for different amounts of DNA in cells. Total fluorescence across the Z-stack was measured for antibody and DAPI, and arbitray units (A.U.) represents the ratio of H2AX and 53BP1 flourescence to DNA in each cell.

Homing Assay

LSM separated BMCs were incubated with biotinylated lineage markers as described above. Then labeled cells were incubated with sheep anti-rat IgG-conjugated magnetic beads (20:1 beads/cell) (Invitrogen, Carlsbad, CA), and Lin-positive (Lin^{+}) cells were removed using a magnetic bead separater. Lin- cells were stained with 5 μM CFSE (Invitrogen) in pre-warmed PBS at 37°C for 20 minutes, washed, and transplanted into 8 Gy irradiated recipients (CD45.1). Recipients were euthanized 2.5 days after BMT and analyzed by flow cytometry for HSPC engraftment.

Serial 5-FU assay

Chimeric mice were generated by transplanting *Id1*$^{-/-}$ and *Id1*$^{+/+}$ BMCs (1×10^{6}) (i.v.) into 10 Gy irradiated recipient mice. Ten weeks after BMT, recipient mice were treated with 5-fluorouracil (5-FU) (135mg/kg), 4 times at 7 day intervals and monitored for survival. Alternatively, chimeric mice were treated with two does of 5-FU (150 mg/kg) separated by 2 weeks. Then 2 weeks after the last injection BMCs were harvested for HSPC immunophenotype analysis (n=5 mice/group), and BMCs (1×10^{6}) were transplanted with competitor BMCs (1×10^{6}) into irradiated (10 Gy) recipient mice to evaluate HSC function. Finally, chimeric *Id1*$^{+/+}$ and *Id1*$^{-/-}$ BMT recipients were treated with 5-FU (135 mg/kg mouse) twice, two weeks apart, and mice were administered BrdU continuously for 3 days

before harvesting BMCs 10 days after the last 5-FU treatment to determine the percentage of BrdU+ HSCs by flow cytometry using the gating strategy shown in Figure S2B.

Mitochondrial activity and ROS measurement

Mononuclear cells were isolated by LSM density gradient separation from *Id1*$^{+/+}$ and *Id1*$^{-/-}$ mice, and from secondary competitive BMT recipient mice after 12 weeks. BMCs (5×10^6 cells/mL) were incubated in StemSpan media (Stem Cell Technologies, Vancouver, CA) at 37°C with either (a) MitoTracker Green (Thermo Fisher Scientific) 50nM for 15 mins, (b) JC-1 (Thermo Fisher Scientific) 2uM for 15 mins, (c) CellRox Deep Red (Thermo Fisher Scientific) 500nM for 30 mins, (d) Thiol tracker violet (Thermo Fisher Scientific) 10μM for 15 mins, or (e) TMRM (Thermo Fisher Scientific) 100nM for 30mins, as per the manufacturer's instructions. Cells were then washed with PBS and stained for HSPC markers, as described above, and analyzed immediately.

In vitro Id1-GFP reporter cell assays

BMCs were harvested from *Id1*$^{GFP/+}$ mice, and LSM separated BMCs, and HSCs, ST-HSCs, MPPsures, common myeloid progenitors (CMP), Lin- c-Kit$^+$ (LK) CD34$^+$ FcR$^-$, granulocyte/macrophage progenitors (GMP), LK CD34$^+$FcR$^+$, megakaryocyte erythroid progenitors (MEP) LK CD34$^-$FcR$^-$, and neutrophils (Mac-1$^+$Gr-1$^+$) were analyzed for GFP expression by flow cytometry. Alternatively, LSM cells were cultured in StemSpan SFEM (Stem Cell Technologies, Vancouver, Canada) serum free medium containing mSCF (100 ng/mL), with or without the additional following cytokines and proinflammatory agents as indicated in the results section: pI:pC 1μg/mL (InvivoGen, San Diego, CA), LPS 1 μg/mL (Sigma, St. Louis, MO), IL-1β 25 ng/mL, IFNγ (type II) 1000 units/mL, IFNα (type I) 1000 units/mL, TNFα 20ng/mL, mIL-3 20 ng/mL, hTPO 100ng/mL, hFLT3L-100 ng/mL, GM-CSF 50 ng/mL, mIL-6 50 ng/mL. All cytokines were from Peprotech, Rocky Hill, NJ. Cells were removed from triplicate cultures after 36 hrs and HSPCs were analyzed for GFP expression by flow cytometry. For BrdU incorporation assays, BMCs were harvested from *Id1*$^{GFP/+}$ reporter mice and Lin- cells were isolated as described above. Lin- cells were cultured for 48 hours in StemSpan along with SCF (100 ng/mL) alone or in combination with TPO (100 ng/mL) and IFNγ (1000 units/mL). The cells were pulsed with 10 μM BrdU (Sigma) for the last 3 hours of the culture, stained with HSPC markers, fixed and permeabilized by Cytofix/Cytoperm buffer (BD Biosciences), treated with DNase and stained with anti-BrdU as per the manufacturer's instructions. Cells were washed with Perm/wash buffer (BD Biosciences) twice and then analyzed by flow cytometry.

In vivo Id1-GFP assays

Irradiation induction of *Id1* expression.—*Id1*$^{GFP/+}$ reporter mice and C57BL/6 controls were exposed to either 0 Gy, 4 Gy, 6 Gy or 8 Gy γIR, and BMCs were harvested 48 and 72 hours after irradiation. BMCs were harvested from treated mice and HSPCs were analyzed for the expression of GFP by flow cytometry as described above.

Cytokine/Growth Factor Induction of *Id1* expression.—BMCs were harvested from *Id1*$^{GFP/+}$ reporter mice (CD45.2$^+$) and were transplanted (1×10^6 cells) into 10 Gy irradiated CD45.1 recipients (chimeric mice). Twenty weeks after BMT chimeric mice (5 mice/group)

were administered, SCF (0.4mg/kg SC), IFNγ (0.43mg/kg IV), mIL6 (0.4mg/kg IP), hTPO (0.4mg/kg SC) (all from Peprotech) or pI:pC (5mg/kg IP) (InvivoGen), or a 6 Gy γIR dose. Recipients and non-transplanted controls were sacrificed 48 hours post-treatment, and BMCs were harvested and HSPCs were analyzed for the expression of GFP as describe above.

JAK/STAT inhibitor effect on *Id1* expression.—C57BL/6 (CD45.1) recipient mice were treated daily for 4 days with either Momelotinib (Selleckchem, Houston, TX) dissolved in 1-methyl-2pyrrolidinone to 120mg/ml and diluted with 0.1M Capsitol to 4mg/ml SC at 22.4 mg/kg, or SH4–54 (Selleckchem) dissolved in 50% polyethylene glycol and 50% PBS IP at 10mg/kg. On day 2, mice were irradiated (8 Gy) and transplanted with 5×10^5 lineage-negative BMCs from $Id1^{GFP/+}$ reporter mice (CD45.2). Recipients were euthanized on day 4 and BMCs were harvested and HSPCs were analyzed for GFP expression as described above.

In vitro culture of hematopoietic stem and progenitor cells

BMCs were harvested from $Id1^{+/+}$ and $Id1^{-/-}$ mice and stained with biotinylated antibodies that recognize lineage markers,and fluorochrome-conjugated streptavidin, and antibodies that recognize c-Kit and Sca-1. LSK cells were purified by FACS and seeded into StemSpan medium containing mSCF (100 ng/mL), hTPO (100 ng/mL), mFGF1 (10ng/mL), hIGF2 (20 ng/mL), and Angiopoietin 2 (50ng/mL) at 3×10^4 cells/ml. Cells were removed from culture after 6 days and analyzed for HSPCs cell cycle using Ki-67/FxCycle, and proliferation using BrdU by flow cytometry as described above. The harvested cells were also analysed for CDKI expression. Briefly, the cells were stained with HSPC surface markers, fixed and permeabilized with BD cytofix/perm buffer, and then stained with p16, p21 and p27 antibodies as described above.

Single cell assay.—BMCs were labled with antibodies that recognize HSPC as described above, and HSCs (LSK $Flk2^{-}CD150^{+}CD48^{-}$) were sorted one cell per well directly into Terasaki plates (Greiner Bio-One) containing StemSpan serum free media supplemented with mSCF plus hTPO, plus mIL-3 (30ng/mL) *in vitro*. Cells were counted at 24, 48 and 60 hours after plating.

Lentiviral mediated shRNA knockdown

Mouse *p16(CDKN2A)* (*SHCLNG-NM_009877), E2a (TCF3)* (*SHCLNG-NM_011548)* shRNA target sequences were purchased from Sigma-Aldrich. Infectious Lentivirus was generated by transfecting the shRNA constructs and packaging plasmids (PMD2G and pCMV8.74) into 293T/17 cells using LipoD293 (SignaGen, Rockville, MD, USA). Virus containing supernatants were collected 48 hours post transfection. To calculate viral titers, NIH3T3 cells were infected with serial dilutions of viral supernatants. For knockdown, lineage depleted cells from mouse bone marrow were transduced with shRNA lentivirus by spinoculation. Lineage depleted cells (Depleted for Mac-1, Gr-1, B220, Ter119, CD4, CD8 and Il7R) were isolated from $Id1^{-/-}$ mice using immune-magnetic bead separation and cultured in Stemspan medium containing mSCF (100 ng/mL), hTPO (100 ng/mL), mFGF1 (10ng/mL), hIGF2 (20 ng/mL), and Angiopoietin 2 (50ng/mL) at 5×10^5 cells/0.5mL for 12

hours. Twelve hours after culture, the cells were subjected to first round of shRNA mediated lentiviral transduction lentivirus, where lineage depleted cells were spun at 2000 x g for 90 minutes at 37°C. The cells were then washed and reseeded with fresh complete medium. After 24 hours, a second round of transduction was performed as described above, and the cells were cultured in puromycin (2 μg/mL). Twenty-four hour after the second lentiviral mediated transduction, the cells were pulsed with 10uM BrdU for 45 min., and then harvested for qRT-PCR and flow cytometry.

RNA-seq analysis

RNA was purified from HSCs isolated from *Id1*$^{-/-}$ and *Id1*$^{+/+}$ mice by flow cytometry as described above, and from HSCs isolated from primary recipient mice 4 weeks after transplantation of Lin- *Id1*$^{-/-}$ and *Id1*$^{+/+}$ BMCs. The SMARTer Ultra Low Input RNA Kit (Thermo Fisher) was used to generate high-quality cDNA. The cDNA was made into a sequencing ready library using the Nextera® XT DNA Sample Preparation Kit (Illumina). The final purified product is then quantitated by qPCR before cluster generation and sequencing on the Illumina HiSeq 2500 sequencer. The HiSeq Real Time Analysis software (RTA 1.18) was used for processing image files, the Illumina CASAVA_v1.8.4 was used for demultiplex and converting binary base calls and qualities to fastq format. The sequencing reads were trimmed for adapters and low quality bases using Trimmomatic (version 0.30). The trimmed reads were aligned to mouse mm9 reference genome (NCBIM37 /UCSC mm9) and Ensembl annotation version 67 using TopHat_v2.0.8 software. Quantification was carried out with RSEM using the transcriptome bam file created by STAR. Differentially expressed genes were obtained by comparing (*Id1*$^{-/-}$ HSCs-stressed - *Id1*$^{-/-}$ HSCs-normal) and (*Id1*$^{+/+}$ HSCs-stressed - *Id1*$^{+/+}$ HSCsnormal). Differentially expressed genes were then analyzed and selected by Limma pipeline with adjusted p value < 0.05, and fold change ± 2 (Table S1).

QUANTIFICATION AND STATISTICAL ANALYSIS

Unless otherwise indicated, data in all figures are expressed as the mean ± SD and are representative of at least 2 trials. Statistical differences between groups was determined by Student’s unpaired t test using Prism 5 software (GraphPad, San Diego, CA). Statistical differences between survival curves were determined using the og-rank (Mant-Cox) test. For all graphs, data are presented as mean ± SD, *P < 0.05, **P < 0.01, ***P < 0.001.

Supplementary Material

Refer to Web version on PubMed Central for supplementary material.

ACKNOWLEDGEMENTS

We wish to thank FNLCR LASP Animal Research and Technical Support Staff, the NCIFrederick Flow Cytometry Core. Dr. Philip Oberdoeffer for his thoughtful review of this manuscript. This project has been funded in part with Federal funds from the Frederick National Laboratory for Cancer Research, NIH, under Contract HHSN261200800001E. The content of this publication does not necessarily reflect the views or policies of the Department of Health and Human Services, nor does mention of trade names, commercial products or organizations imply endorsements by the US Government.

REFERENCES

Baldridge MT, King KY, Boles NC, Weksberg DC, and Goodell MA (2010). Quiescent haematopoietic stem cells are activated by IFN-gamma in response to chronic infection. Nature 465, 793–797. [PubMed: 20535209]

Beerman I, Bhattacharya D, Zandi S, Sigvardsson M, Weissman IL, Bryder D, and Rossi DJ (2010a). Functionally distinct hematopoietic stem cells modulate hematopoietic lineage potential during aging by a mechanism of clonal expansion. Proc Natl Acad Sci U S A 107, 5465–5470. [PubMed: 20304793]

Beerman I, Bock C, Garrison BS, Smith ZD, Gu H, Meissner A, and Rossi DJ (2013). Proliferation-dependent alterations of the DNA methylation landscape underlie hematopoietic stem cell aging. Cell Stem Cell 12, 413–425. [PubMed: 23415915]

Beerman I, Maloney WJ, Weissmann IL, and Rossi DJ (2010b). Stem cells and the aging hematopoietic system. Current opinion in immunology 22, 500–506. [PubMed: 20650622]

Branzei D, and Foiani M (2010). Maintaining genome stability at the replication fork. Nature reviews Molecular cell biology 11, 208–219. [PubMed: 20177396]

Cheng T, Rodrigues N, Shen H, Yang Y, Dombkowski D, Sykes M, and Scadden DT (2000). Hematopoietic stem cell quiescence maintained by p21cip1/waf1. Science 287, 1804–1808. [PubMed: 10710306]

Cochrane SW, Zhao Y, Perry SS, Urbaniak T, and Sun XH (2011). Id1 has a physiological role in regulating early B lymphopoiesis. Cellular & molecular immunology 8, 41–49. [PubMed: 21200383]

Cochrane SW, Zhao Y, Welner RS, and Sun XH (2009). Balance between Id and E proteins regulates myeloid-versus-lymphoid lineage decisions. Blood 113, 1016–1026. [PubMed: 18927439]

Dahlberg A, Delaney C, and Bernstein ID (2011). Ex vivo expansion of human hematopoietic stem and progenitor cells. Blood 117, 6083–6090. [PubMed: 21436068]

Dykstra B, Olthof S, Schreuder J, Ritsema M, and de Haan G (2011). Clonal analysis reveals multiple functional defects of aged murine hematopoietic stem cells. J Exp Med 208, 2691–2703. [PubMed: 22110168]

Esplin BL, Shimazu T, Welner RS, Garrett KP, Nie L, Zhang Q, Humphrey MB, Yang Q, Borghesi LA, and Kincade PW (2011). Chronic exposure to a TLR ligand injures hematopoietic stem cells. J Immunol 186, 5367–5375. [PubMed: 21441445]

Flach J, Bakker ST, Mohrin M, Conroy PC, Pietras EM, Reynaud D, Alvarez S, Diolaiti ME, Ugarte F, Forsberg EC, et al. (2014). Replication stress is a potent driver of functional decline in ageing haematopoietic stem cells. Nature 512, 198–202. [PubMed: 25079315]

Geiger H, de Haan G, and Florian MC (2013). The ageing haematopoietic stem cell compartment. Nature reviews Immunology 13, 376–389.

Gekas C, and Graf T (2013). CD41 expression marks myeloid-biased adult hematopoietic stem cells and increases with age. Blood 121, 4463–4472. [PubMed: 23564910]

Harrison DE, and Lerner CP (1991). Most primitive hematopoietic stem cells are stimulated to cycle rapidly after treatment with 5-fluorouracil. Blood 78, 1237–1240. [PubMed: 1878591]

Ichii M, Shimazu T, Welner RS, Garrett KP, Zhang Q, Esplin BL, and Kincade PW (2010). Functional diversity of stem and progenitor cells with B-lymphopoietic potential. Immunol Rev 237, 10–21. [PubMed: 20727026]

Ito K, Hirao A, Arai F, Takubo K, Matsuoka S, Miyamoto K, Ohmura M, Naka K, Hosokawa K, Ikeda Y, et al. (2006). Reactive oxygen species act through p38 MAPK to limit the lifespan of hematopoietic stem cells. Nature medicine 12, 446–451.

Jankovic V, Ciarrocchi A, Boccuni P, DeBlasio T, Benezra R, and Nimer SD (2007). Id1 restrains myeloid commitment, maintaining the self-renewal capacity of hematopoietic stem cells. Proc Natl Acad Sci U S A 104, 1260–1265. [PubMed: 17227850]

Kee BL (2009). E and ID proteins branch out. Nature reviews Immunology 9, 175–184.

Kim JH, Jenrow KA, and Brown SL (2014). Mechanisms of radiation-induced normal tissue toxicity and implications for future clinical trials. Radiation oncology journal 32, 103–115. [PubMed: 25324981]

Koni PA, Joshi SK, Temann UA, Olson D, Burkly L, and Flavell RA (2001). Conditional vascular cell adhesion molecule 1 deletion in mice: impaired lymphocyte migration to bone marrow. J Exp Med 193, 741–754. [PubMed: 11257140]

Lasorella A, Benezra R, and Iavarone A (2014). The ID proteins: master regulators of cancer stem cells and tumour aggressiveness. Nature reviews Cancer 14, 77–91. [PubMed: 24442143]

Leeanansaksiri W, Wang H, Gooya JM, Renn K, Abshari M, Tsai S, and Keller JR (2005). IL-3 induces inhibitor of DNA-binding protein-1 in hemopoietic progenitor cells and promotes myeloid cell development. J Immunol 174, 7014–7021. [PubMed: 15905544]

Ling F, Kang B, and Sun XH (2014). Id proteins: small molecules, mighty regulators. Current topics in developmental biology 110, 189–216. [PubMed: 25248477]

Markus T, Cronberg T, Cilio C, Pronk C, Wieloch T, and Ley D (2009). Tumor necrosis factor receptor-1 is essential for LPS-induced sensitization and tolerance to oxygen-glucose deprivation in murine neonatal organotypic hippocampal slices. Journal of cerebral blood flow and metabolism : official journal of the International Society of Cerebral Blood Flow and Metabolism 29, 73–86.

Matatall KA, Jeong M, Chen S, Sun D, Chen F, Mo Q, Kimmel M, and King KY (2016). Chronic Infection Depletes Hematopoietic Stem Cells through Stress-Induced Terminal Differentiation. Cell reports 17, 2584–2595. [PubMed: 27926863]

Mendelson A, and Frenette PS (2014). Hematopoietic stem cell niche maintenance during homeostasis and regeneration. Nature medicine 20, 833–846.

Morrison SJ, and Scadden DT (2014). The bone marrow niche for haematopoietic stem cells. Nature 505, 327–334. [PubMed: 24429631]

Nakamura-Ishizu A, Takizawa H, and Suda T (2014). The analysis, roles and regulation of quiescence in hematopoietic stem cells. Development 141, 4656–4666. [PubMed: 25468935]

Orkin SH, and Zon LI (2008). Hematopoiesis: an evolving paradigm for stem cell biology. Cell 132, 631–644. [PubMed: 18295580]

Pellegrino S, Michelena J, Teloni F, Imhof R, and Altmeyer M (2017). Replication-Coupled Dilution of H4K20me2 Guides 53BP1 to Pre-replicative Chromatin. Cell reports 19, 1819–1831. [PubMed: 28564601]

Perk J, Iavarone A, and Benezra R (2005). Id family of helix-loop-helix proteins in cancer. Nature reviews Cancer 5, 603–614. [PubMed: 16034366]

Perry SS, Zhao Y, Nie L, Cochrane SW, Huang Z, and Sun XH (2007). Id1, but not Id3, directs long-term repopulating hematopoietic stem-cell maintenance. Blood 110, 2351–2360. [PubMed: 17622570]

Pietras EM, Mirantes-Barbeito C, Fong S, Loeffler D, Kovtonyuk LV, Zhang S, Lakshminarasimhan R, Chin CP, Techner JM, Will B, et al. (2016). Chronic interleukin-1 exposure drives haematopoietic stem cells towards precocious myeloid differentiation at the expense of selfrenewal. Nature cell biology 18, 607–618. [PubMed: 27111842]

Qiu J, Papatsenko D, Niu X, Schaniel C, and Moore K (2014). Divisional history and hematopoietic stem cell function during homeostasis. Stem cell reports 2, 473–490. [PubMed: 24749072]

Rodrigues-Moreira S, Moreno SG, Ghinatti G, Lewandowski D, Hoffschir F, Ferri F, Gallouet AS, Gay D, Motohashi H, Yamamoto M, et al. (2017). Low-Dose Irradiation Promotes Persistent Oxidative Stress and Decreases Self-Renewal in Hematopoietic Stem Cells. Cell reports 20, 3199–3211. [PubMed: 28954235]

Roschger C, and Cabrele C (2017). The Id-protein family in developmental and cancer-associated pathways. Cell Commun Signal 15, 7. [PubMed: 28122577]

Sawen P, Lang S, Mandal P, Rossi DJ, Soneji S, and Bryder D (2016). Mitotic History Reveals Distinct Stem Cell Populations and Their Contributions to Hematopoiesis. Cell reports 14, 2809–2818. [PubMed: 26997272]

Schaue D, Kachikwu EL, and McBride WH (2012). Cytokines in radiobiological responses: a review. Radiation research 178, 505–523. [PubMed: 23106210]

Schaue D, Micewicz ED, Ratikan JA, Xie MW, Cheng G, and McBride WH (2015). Radiation and inflammation. Seminars in radiation oncology 25, 4–10. [PubMed: 25481260]

Seita J, and Weissman IL (2010). Hematopoietic stem cell: self-renewal versus differentiation. Wiley interdisciplinary reviews Systems biology and medicine 2, 640–653. [PubMed: 20890962]

Semerad CL, Mercer EM, Inlay MA, Weissman IL, and Murre C (2009). E2A proteins maintain the hematopoietic stem cell pool and promote the maturation of myelolymphoid and myeloerythroid progenitors. Proc Natl Acad Sci U S A 106, 1930–1935. [PubMed: 19181846]

Suh HC, Ji M, Gooya J, Lee M, Klarmann KD, and Keller JR (2009). Cell-nonautonomous function of Id1 in the hematopoietic progenitor cell niche. Blood 114, 1186–1195. [PubMed: 19478045]

Suh HC, Leeanansaksiri W, Ji M, Klarmann KD, Renn K, Gooya J, Smith D, McNiece I, Lugthart S, Valk PJ, et al. (2008). Id1 immortalizes hematopoietic progenitors in vitro and promotes a myeloproliferative disease in vivo. Oncogene 27, 5612–5623. [PubMed: 18542061]

Sukumar M, Liu J, Mehta GU, Patel SJ, Roychoudhuri R, Crompton JG, Klebanoff CA, Ji Y, Li P, Yu Z, et al. (2016). Mitochondrial Membrane Potential Identifies Cells with Enhanced Stemness for Cellular Therapy. Cell metabolism 23, 63–76. [PubMed: 26674251]

Trumpp A, Essers M, and Wilson A (2010). Awakening dormant haematopoietic stem cells. Nature reviews Immunology 10, 201–209.

Vannini N, Girotra M, Naveiras O, Nikitin G, Campos V, Giger S, Roch A, Auwerx J, and Lutolf MP (2016). Specification of haematopoietic stem cell fate via modulation of mitochondrial activity. Nature communications 7, 13125.

Wahlestedt M, Pronk CJ, and Bryder D (2015). Concise review: hematopoietic stem cell aging and the prospects for rejuvenation. Stem cells translational medicine 4, 186–194. [PubMed: 25548388]

Walasek MA, van Os R, and de Haan G (2012). Hematopoietic stem cell expansion: challenges and opportunities. Annals of the New York Academy of Sciences 1266, 138–150. [PubMed: 22901265]

Walter D, Lier A, Geiselhart A, Thalheimer FB, Huntscha S, Sobotta MC, Moehrle B, Brocks D, Bayindir I, Kaschutnig P, et al. (2015). Exit from dormancy provokes DNA-damage-induced attrition in haematopoietic stem cells. Nature 520, 549–552. [PubMed: 25707806]

Wang LH, and Baker NE (2015). E Proteins and ID Proteins: Helix-Loop-Helix Partners in Development and Disease. Developmental cell 35, 269–280. [PubMed: 26555048]

Yang Q, Esplin B, and Borghesi L (2011). E47 regulates hematopoietic stem cell proliferation and energetics but not myeloid lineage restriction. Blood 117, 3529–3538. [PubMed: 21273306]

Zhang H, Rodriguez S, Wang L, Wang S, Serezani H, Kapur R, Cardoso AA, and Carlesso N (2016). Sepsis Induces Hematopoietic Stem Cell Exhaustion and Myelosuppression through Distinct Contributions of TRIF and MYD88. Stem cell reports 6, 940–956. [PubMed: 27264973]

Highlights

- *Id1*$^{-/-}$ HSCs have enhanced self-renewal potential and are maintained during BMT
- *Id1*$^{-/-}$ HSCs show reduced oxidative stress and increased quiescence after BMT
- *Id1*$^{-/-}$ HSCs are protected from inflammatory cytokine-induced proliferative stress
- *Id1*$^{-/-}$ HSCs are protected from exhaustion by chronic inflammatory stress and aging

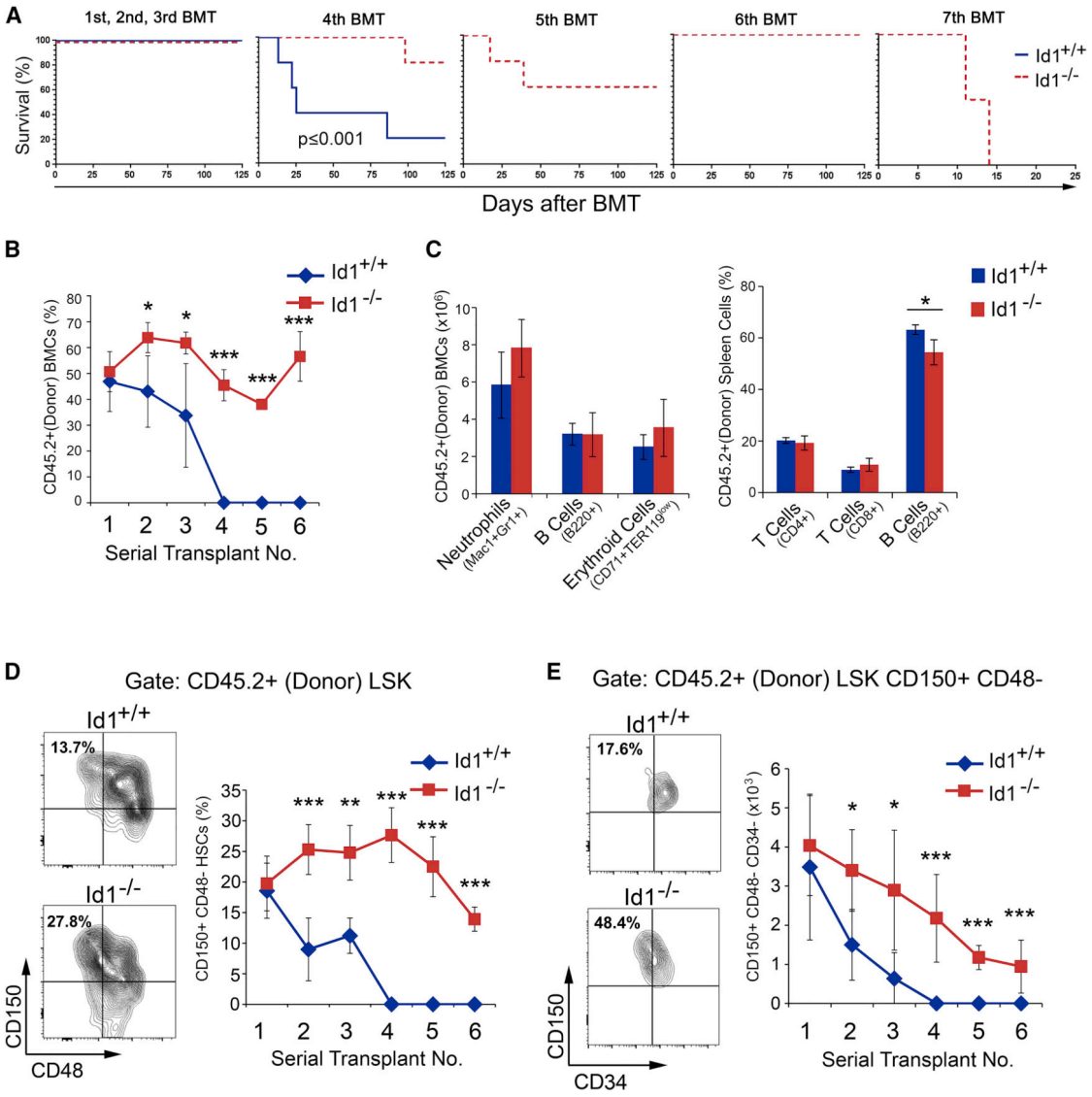

Figure 1. Ablation of *Id1* enhances self-renewal of HSCs.

(A) Kaplan-Meier survival curves of mice competitively transplanted with $Id1^{+/+}$ and $Id1^{-/-}$ BMCs. (B) Percentage of donor-derived ($CD45.2^{+}$) BMCs in serially transplanted recipients. (C) Quantitation of of lineage repopulation in BM and spleen cells from primary BMT recipient mice. (D) Frequency of donor-derived $Id1^{-/-}$ and $Id1^{+/+}$ HSCs in serial BMT recipient mice. using the gating strategy in Figure S2B. (E) Total number of donor-derived $Id1^{-/-}$ and $Id1^{+/+}$ HSCs in serial BMT recipient mice. Representative FACS analysis of donor HSCs in BMCs from secondary BMT recipient mice (left). See also Figure S1/S2.

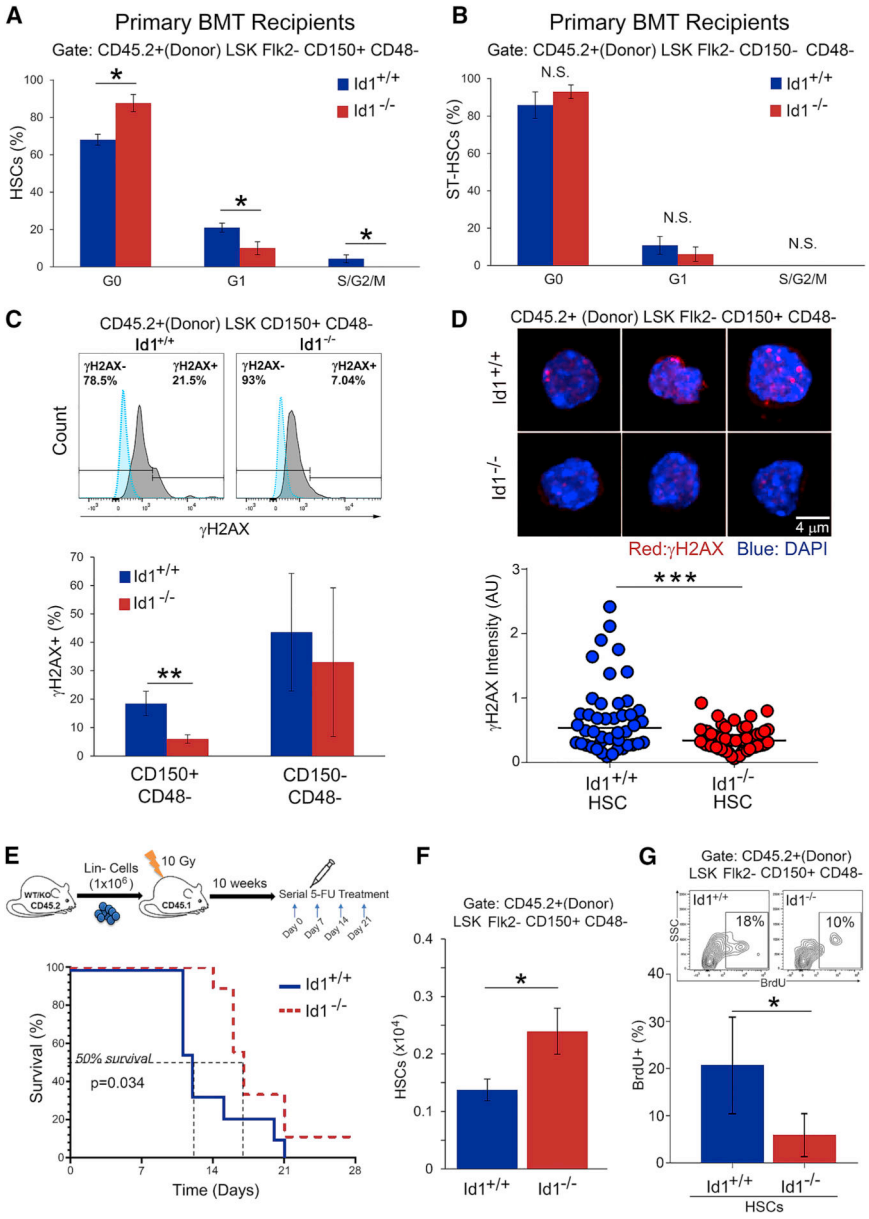

Figure 2. Increased quiescence of *Id1*$^{-/-}$ HSCs after bone marrow transplantation.

(A-B) Quantitation of *Id1*$^{-/-}$ and *Id1*$^{+/+}$ HSC cycling in primary recipient mice by Ki-67/ FxCycle analysis. (n=5 mice/group). (C) Quantitation of γH2AX phosphorylation expression levels of *Id1*$^{-/-}$ and *Id1*$^{+/+}$ HSC in primary BMT recipient mice by flow cytometry (n=5 mice/group). (D) Immunoflourescence analysis of γ-H2AX foci in *Id1*$^{-/-}$ and *Id1*$^{+/+}$ HSCs FACS sorted from primary BMT recipient mice by confocal microscopy. Mann-Witney test p<0.00086, and z-score −3.33. (E) Kaplan-Meier survival curves of chimeric *Id1*$^{+/+}$ and *Id1*$^{-/-}$ recipient mice treated with 5-FU. Mantel-Cox test P=0.034 (n=10 mice/group). (F) Quanitification of HSCs in chimeric *Id1*$^{+/+}$ and *Id1*$^{-/-}$ BMT recipient mice treated with 5-FU (n=5 mice/group). (G) Quantification of HSC proliferation in *Id1*$^{-/-}$ and *Id1*$^{+/+}$ chimeric mic after 5-FU-induced proliferative stress by BrdU incorporation assay (n=5 mice/group). See also Figure S3/S4.

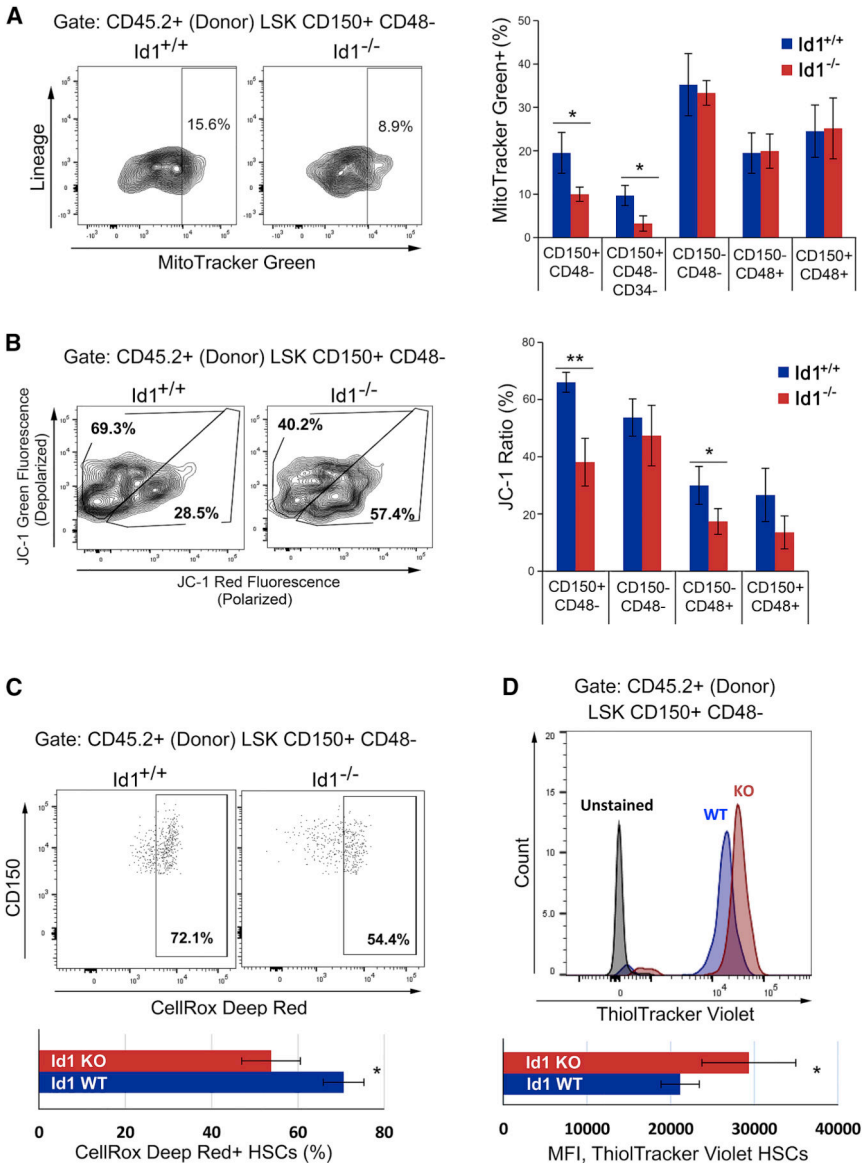

Figure 3. Reduced mitochondrial stress and ROS production in *Id1*$^{-/-}$ HSCs after bone marrow transplantation.

(A) Quantification of mitochondrial biogenesis in *Id1*$^{-/-}$ and *Id1*$^{+/+}$ HSPCs from secondary BMT recipients using MitoTracker Green and flow cytometry(n=5 mice/group). (B) Quantification of mitochondrial stress in *Id1*$^{-/-}$ and *Id1*$^{+/+}$ HSCs from secondary BMT recipients using JC-1 to measure mitochondrial membrane depolarization. (Percentage JC-1 ratios = % FITC/(% FITC $^{+}$ % PE) x100) (n=5 mice/group). (C) ROS expression levels in *Id1*$^{-/-}$ and *Id1*$^{+/+}$ HSCs from secondary BMT recipients using CellRox Deep Red (n=5 mice/group). (D) Quantification of intracellular reduced thiols in *Id1*$^{-/-}$ and *Id1*$^{+/+}$ HSCs from secondary BMT recipients using ThiolTraker Violet (n=5 mice/group). See also Figure S5.

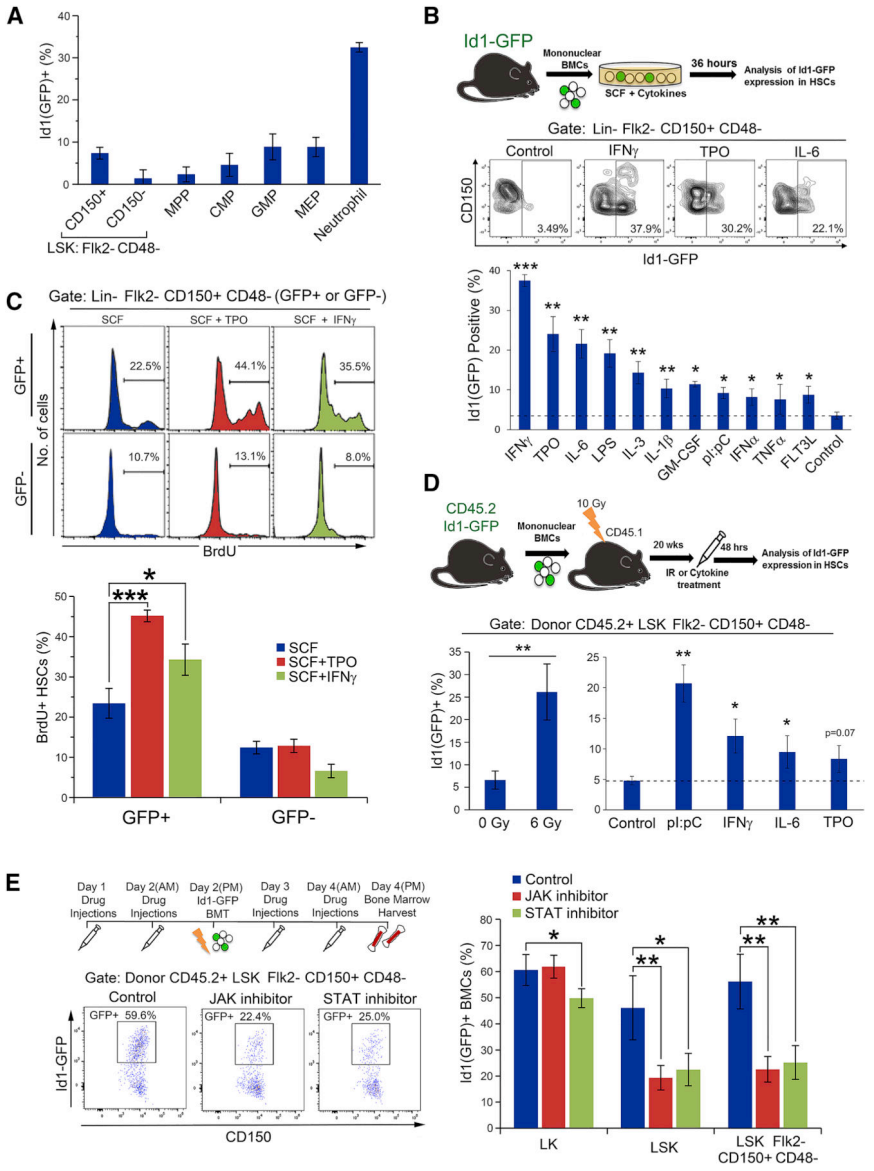

Figure 4. *Id1* expression is upregulated in hematopoietic stem and progenitor cells by cytokines and proinflammatory agents.

(A) Expression of Id1(GFP) in HSPCs in *Id1*$^{GFP/+}$ mice (n=5 mice/group). **(B)** Cytokine/growth factor induced Id1(GFP) expression in HSCs from Lin- *Id1*$^{GFP/+}$ reporter BMC cultures. Dashed line indicates percent Id1(GFP) expression for cells cultured in SCF alone. **(C)** Cytokine/growth factor induced proliferation of Id1(GFP^{+}) and Id1(GFP^{-}) HSCs from Lin- *Id1*$^{GFP/+}$ reporter BMC cultures. **(D)** γ-irradiation, cytokines and proinflammatory mediator induction of Id1(GFP) expression in HSCs from *Id1*$^{GFP/+}$ reporter BMCs *in vivo*. Dashed lined indicates control value for mice treated with saline (n=5 mice/group). **(E)** Effect of pan-JAK and pan-STAT inhibitors on the induction of Id1(GFP) expression in HSCs following BMT of *Id1*$^{GFP/+}$ reporter BMCs. (n=5 mice/group). See also Figure S6.

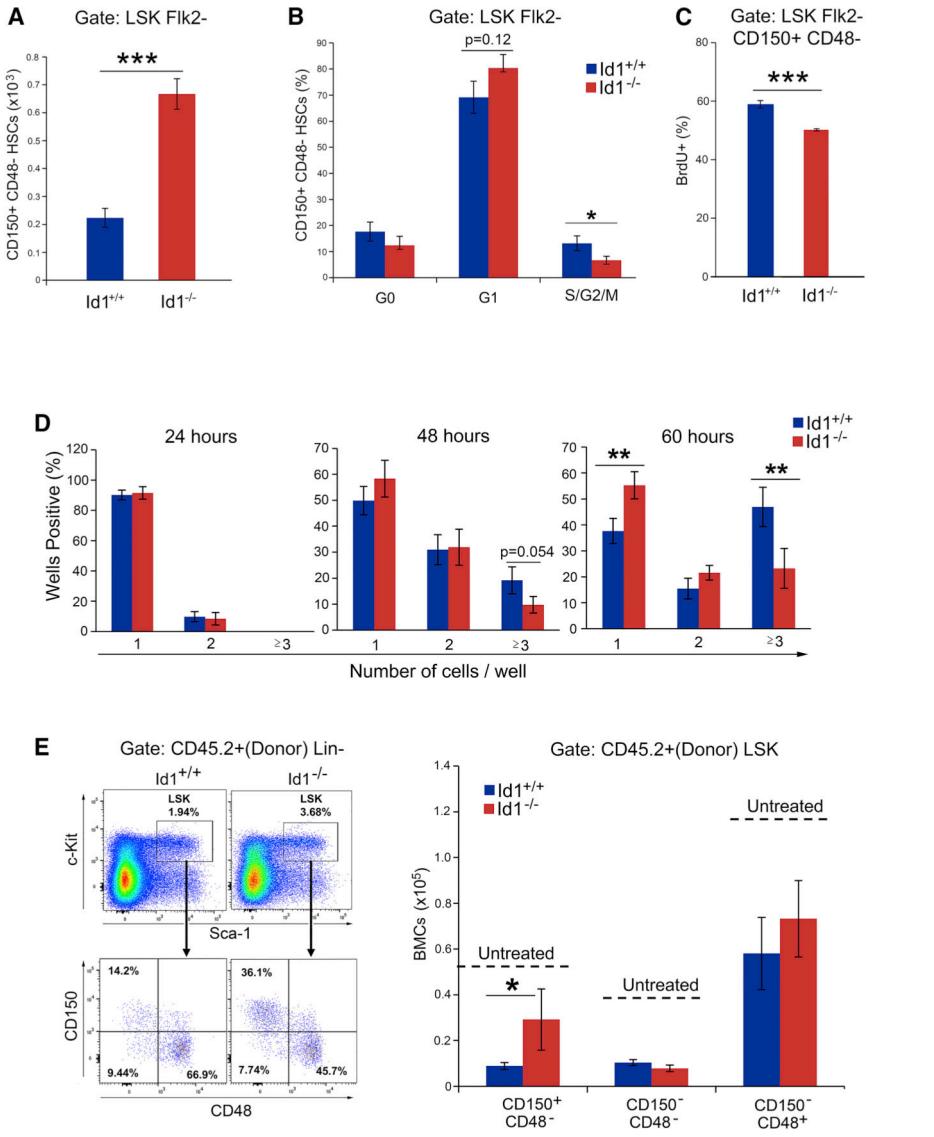

Figure 5. Increased survival and quiescence of *Id1*$^{-/-}$ HSCs *in vitro*.

(A) Total number of HSCs present in *Id1*$^{+/+}$ and *Id1*$^{-/-}$ LSK cell cultures after 6 days in vitro culture. **(B)** HSC cycling in LSK cell cultures after 6 days determined by Ki-67/FxCycle staining, and **(C)** proliferation by BrdU incorporation. **(D)** HSC single cell division assay. **(E)** Total number of HSCs in *Id1*$^{-/-}$ and *Id1*$^{-/-}$ chimeric mice treated with LPS (0.043 mg/kg) every other day for 30 days (n=5 mice/group). Dashed lines indicate values from untreated control mice. See Figure S6C.

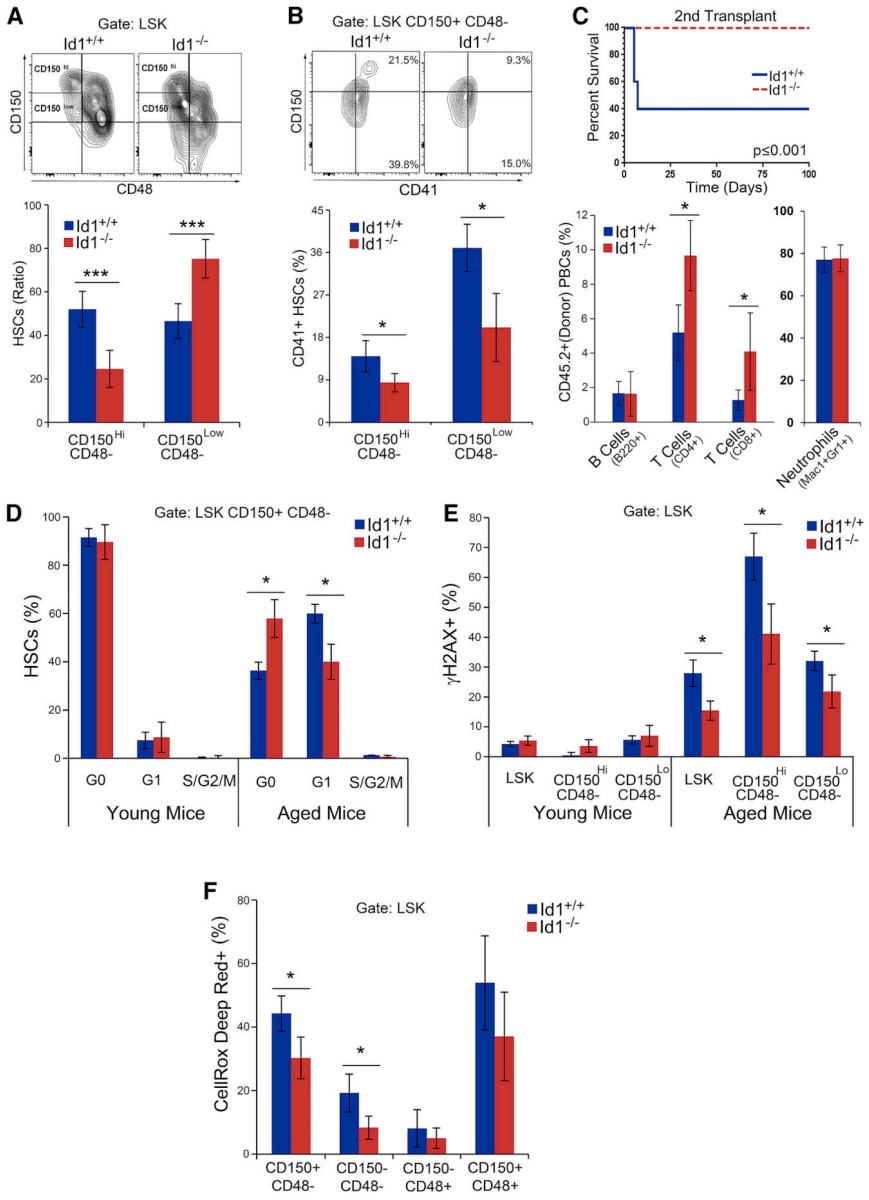

Figure 6. Reduced aging of *Id1*$^{-/-}$ HSCs *in vivo*.

(A) CD150^{Hi} and CD150^{Lo} HSCs in aged (2 year) *Id1*$^{+/+}$ and *Id1*$^{-/-}$ HSCs from *Tie2;Id1*$^{-/-}$ and *Tie2;Id1*$^{+/+}$ mice. HSC Ratio calculated as [(% CD150^{Hi}/ % CD150^{Hi} + %CD150^{Lo}) x 100)] (n=4 mice/group). (B) Expression of CD41 on aged CD150^{Hi} and CD150^{Lo} *Id1*$^{-/-}$ and *Id1*$^{+/+}$ HSCs. (C) Kaplan-Meier survival curves of secondary BMT recipients of 100 FACS sorted aged *Id1*$^{-/-}$ and *Id1*$^{+/+}$ HSCs (Mantel-Cox Test P <0.05), and donor cell repopulation in PBCs from primary recipient mice after 4 months (n=5 mice/group) (D) Cell cycling of aged and young (2 month) HSCs (n=4 mice/group). (E) Percentage of CD150^{Hi} and CD150^{Lo} HSCs from aged and young mice that express phosphorylated γH2AX (n=4 mice/group). (F) Percentage CellRox Deep Red^{+} HSCs, ST-HSCs and MPPs from aged and young mice (n=4 mice/group). See also Figure S7.

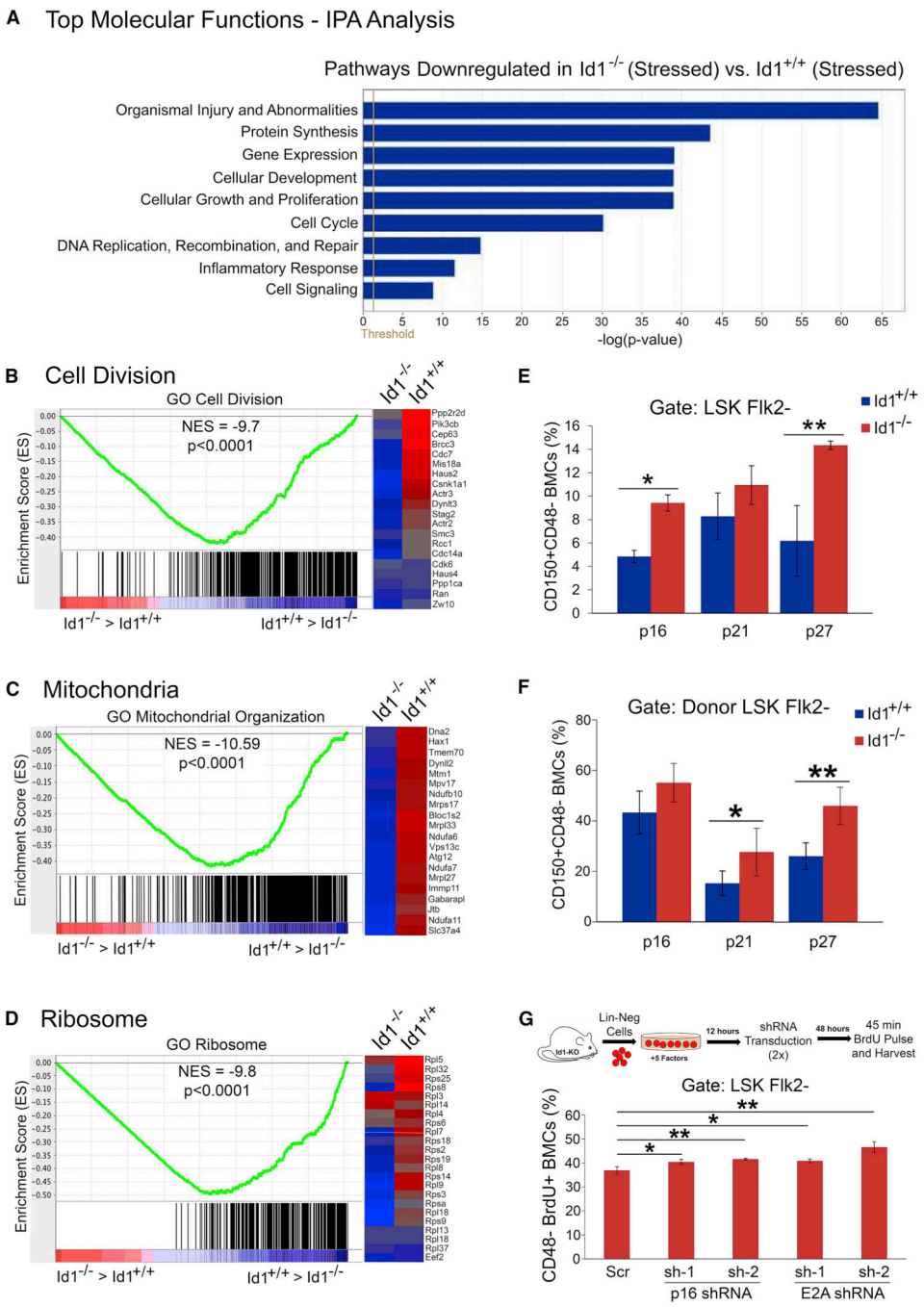

Figure 7.

Quiescent Molecular Signature of *Id1*$^{-/-}$ HSCs after bone marrow transplantation.

(A) IPA analysis of differentially expressed genes revealed the top molecular functions affected by loss of *Id1* in HSCs. All pathways were significantly downregulated in *Id1*$^{-/-}$ HSCs. GSEA analysis of differentially expressed genes shows **(B)** a reduction in GO Cell Division genes in *Id1*$^{-/-}$ HSC compared to *Id1*$^{+/+}$ HSCs, **(C)** a reduction in GO Mitochondrial Organization genes that regulate mitochondrial biogenesis and oxidative phosphorylation in *Id1*$^{-/-}$ HSCs compared to *Id1*$^{+/+}$ HSCs, and **(D)** a reduction in GO

Ribosome genes that regulate ribosomal function in *Id1*$^{-/-}$ HSCs compared to *Id1*$^{+/+}$ HSCs. Heat maps on the right side of enrichment plots show expression of some of the gene hits in the enrichment plots that are up or down downregulated in *Id1*$^{-/-}$ HSCs following BMT (blue/red indicates low/high level of gene expression). **(E)** Expression of p16, p21 and p27 in Id1$^{-/-}$ and Id1$^{+/+}$ HSCs in Lin- expansion assays after 6 days determined by flow cytometry. **(F)** Expression of p16, p21 and p27 in BMCs were harvested from mice competitively transplanted with *Id1*$^{-/-}$ and *Id1*$^{+/+}$ HSCs after 14 wks (n=5/mice group). **(G)** Proliferation of *Id1*$^{-/-}$ and *Id1*$^{+/+}$ HSCs in Lin- cell expansion assays after knockdown of *p16* and *E2A* expression by BrdU incorporation. See also Figure S7.